PACIFIC EARTHQUAKE ENGINEERING RESEARCH CENTER

A Nonlinear Kinetic Model for Multi-Stage Friction Pendulum Systems

Paul L. Drazin
Sanjay Govindjee

Department of Civil and Environmental Engineering
University of California, Berkeley

PEER Report No. 2017/07
Pacific Earthquake Engineering Research Center
Headquarters at the University of California, Berkeley

October 2017

PEER 2017/07
October 2017

A Nonlinear Kinetic Model for Multi-Stage Friction Pendulum Systems

Paul L. Drazin

Sanjay Govindjee

Department of Civil and Environmental Engineering
University of California, Berkeley

PEER Report 2017/07
Pacific Earthquake Engineering Research Center
Headquarters at the University of California, Berkeley

October 2017

ABSTRACT

Multi-stage friction pendulum systems (MSFPs), or more specifically the triple friction pendulum (TFP), are currently being developed as seismic isolation devices for buildings and other large structures. However, all current models are inadequate in properly modeling all facets of these devices. Either the model can only handle uni-directional ground motions while incorporating the kinetics of the TFP system, or the model ignores the kinetics and only models bi-directional motion. And in all cases, the model is linearized to simplify the equations.

This paper presents an all-in-one model that incorporates the full nonlinear kinetics of the TFP system while allowing for bi-directional ground motion. In this way, the model presented here is the most complete single model currently available. The model is developed in such a way that allows for easy expansion to any standard type of MSFP, simply by following the procedure outlined in this paper.

It was found that the nonlinear model can more accurately predict the experimental results for large displacements due to the nonlinear kinematics used to describe the system. It is also shown that the inertial effects of TFP system are negligible in normal operating regimes, however, in the event of uplift, the inertial effects may become significant. The model is also able to accurately predict the experimental results for complicated bi-directional ground motions.

ACKNOWLEDMENTS

This work was supported by the State of California through the Transportation Systems Research Program of the Pacific Earthquake Engineering Research Center (PEER). Any opinions, findings, and conclusions or recommendations expressed in this material are those of the authors and do not necessarily reflect those of the funding agency.

CONTENTS

LIST OF TABLES

LIST OF FIGURES

1 Introduction

Multi-stage friction pendulum systems (MSFPs) are currently being designed and developed as seismic isolation devices for a wide range of structural and non-structural systems [Mokha et al. 1996; Warn and Ryan 2012; and Zayas and Low 1999]. One of the earliest forms of the MSFP was the single friction pendulum developed by Zayas et al. [1987]. This original design has been expanded to double and triple friction pendulums to increase the utility of the device as a seismic isolator [Fadi and Constantinou 2010; Fenz and Constantinou 2008c]. These seismic isolators consist of steel bearings with spherical concave surfaces that slide along one another. An example of the triple friction pendulum (TFP) can be seen in Figure 1.1. As the bearings slide along one another, they are able to provide restoring forces related to the relative displacement between bearings, which creates a variable stiff- ness associated with the overall motion of the friction pendulum [Fadi and Constantinou 2010]. Also, the friction between sliding bearings gives the friction pendulums a hysteretic behavior [Fenz and Constantinou 2008c].

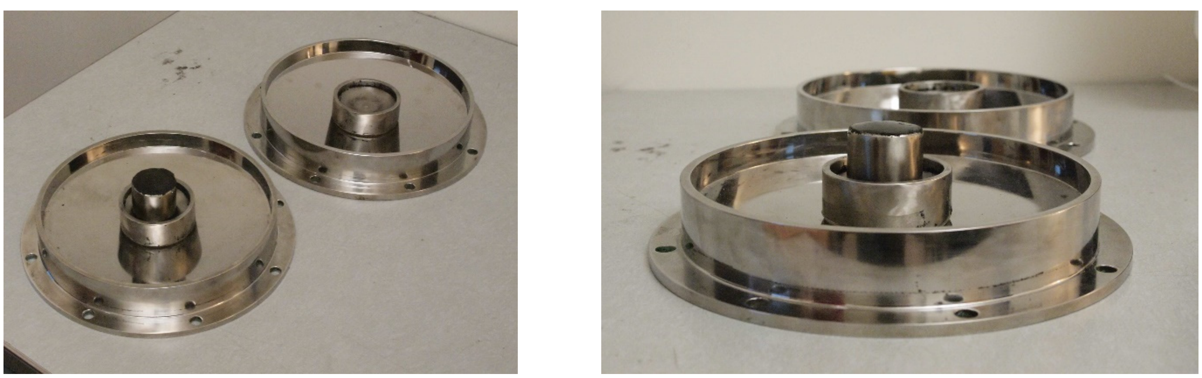

(a) (b)

Figure 1.1 (a) An overview image of an example of a Triple Friction Pendulum (TFP); and (b) a close up front view of a TFP.

Multiple areas of the world, including California and Japan, are at a constant risk from a major earthquake, and the proper usage of seismic isolators, such as MSFPs, can drastically reduce the damage sustained by buildings, bridges, etc. due to strong ground motion [Constantinou et al. 2007; Morgan and Mahin 2010]. For this reason, well-functioning models of MSFPs are necessary to make sure that structures are properly isolated in the event of an earthquake. As the usage of MSFPs has become more common, extensive experimental tests on MSFPs have been undertaken to help characterize their motion due to different types of excitation [Fenz and Constantinou 2008b; Mosqueda et al. 2004]. However, experimental tests can be expensive and time consuming; thus numerical models were developed to simulate the behavior of these MSFPs [Becker and Mahin 2013a; Becker and Mahin 2013b; Fenz and Constantinou 2008a; and Tsai et al. 2010]. While current models have come a long way, no current model for MSFPs utilizes a rigorous setup for the kinematics of the internal sliders; they start directly with scalar equations. Another drawback of current models is that no single model incorporates the full kinetics of the MSFPs with bi-directional motion; they model either the full kinetics for uni-directional motion or the bi-directional motion with only kinematics and no kinetics.

This paper aims to expand upon the current models for Multi-Stage Friction Pendulum systems (MSFPs), which will incorporate the full kinetics, with no linearization as-assumptions and no restrictions on the overall motion. A rigorous use of vectors to describe the kinematics of the internal sliders will help to clarify the overall motion of MSFPs. This will also aid in the setup of the kinetics of the MSFPs, as well as facilitating the modeling of multi-directional motion. The model presented herein will incorporate full vectorially described motion with trajectories constrained to the configuration manifold as defined by mathematically-precise constraints.

Constructing the model in this way directly facilitates a number of modeling advances and naturally leads to robust numerical approximations. The advantages of the model are as follows: (1) it will be a geometrically fully nonlinear model; (2) it will be able to naturally handle multi-directional motions, including complex rotary motions on the sliding surfaces, top and bottom plate rotations, etc.; (3) by construction, it will be fully dynamic and allow for rate dependent analysis; and (4) it will be modular and permit the use of advanced friction models. This paper will apply the vectorized motion to that of the triple friction pendulum system, a type of MSFP, as a benchmark for the new model, but it will be done in such a way that allows for easy expansion to other, more complicated MSFP systems.

2 Triple Friction Pendulum: Equations of Motion

First, the equations of motion for the TFP are defined. In doing so, the patterns in the equations will clearly demonstrate they can be easily expanded to more complicated MSFPs. Figure 2.1 shows a cross-sectional view of the TFP used in this paper.

2.1 KINEMATICS

In order to define the equations of motion, the position vectors of all of the important locations in the TFP need to be defined, such as the center-of-mass of each bearing. Each bearing will have its own set of co-rotational basis vectors defined using sets of 1-2-3 Euler angles [O'Reilly 2008], all relative to the previous bearing. It is worth noting that the Euler angle singularity for the 1-2-3 set occurs when the second rotation angle—in this paper defined as θ_α—is equal to $\pm\frac{\pi}{2}$ [O'Reilly 2008]. In order to avoid this singularity, θ_α is restricted to $\theta_\alpha \in \left(-\frac{\pi}{2}, \frac{\pi}{2}\right)$, which is well within the operating regime of MSFPs. By taking advantage of the axial symmetry of the bearings, only the 1-2 Euler angles are needed to define the basis vectors. Figure 2.2 shows graphically how the basis vectors are constructed from 1-2-3 Euler angles for the first set of Euler angles. The co-rotational bases are defined as:

$$\mathbf{t}_i^1 = \mathbf{R}_1 \mathrm{E}_i, \quad \mathbf{t}_i^2 = \mathbf{R}_2 \mathbf{t}_i^1, \quad \mathbf{t}_i^3 = \mathbf{R}_3 \mathbf{t}_i^2, \quad \mathbf{t}_i^4 = \mathbf{R}_4 \mathbf{t}_i^3, \quad \mathbf{t}_i^5 = \mathbf{R}_5 \mathbf{t}_i^4 \tag{2.1}$$

with the following rotation tensors

$$\begin{aligned} &\mathbf{R}_1 = \mathbf{R}\left(\psi_1, \theta_{1,} \mathrm{E}_i\right), \quad \mathbf{R}_2 = \mathbf{R}\left(\psi_2, \theta_{2,} \mathbf{t}_i^1\right) \quad \mathbf{R}_3 = \mathbf{R}\left(\psi_3, \theta_{3,} \mathbf{t}_i^2\right) \\ &\mathbf{R}_4 = \mathbf{R}\left(\psi_4, \theta_{4,} \mathbf{t}_i^3\right) \quad \mathbf{R}_5 = \mathbf{R}\left(\psi_5, \theta_{5,} \mathbf{t}_i^4\right) \end{aligned} \tag{2.2}$$

Each rotation tensor can be broken down into a series of two rotations as follows:

$$\mathbf{R}\left(\psi_1, \theta_1, \mathbf{E}_i\right) = \mathbf{L}_2\left(\theta_1, \mathbf{t}_i^{1'}\right) \mathbf{L}_1\left(\psi_1, \mathbf{E}_i\right) \tag{2.3}$$

where the individual rotations have the following definitions

$$\mathbf{L}_1\left(\psi_1,\mathbf{E}_i\right)=\cos\left(\psi_1\right)\left(\mathbf{E}_2\otimes\mathbf{E}_2+\mathbf{E}_3\otimes\mathbf{E}_3\right)+\sin\left(\psi_1\right)\left(\mathbf{E}_3\otimes\mathbf{E}_2-\mathbf{E}_2\otimes\mathbf{E}_3\right)+\mathbf{E}_1\otimes\mathbf{E}_1 \quad (2.4)$$

and

$$\mathbf{L}_2\left(\theta_1,\mathbf{t}_i^{1'}\right)=\cos\left(\theta_1\right)\left(\mathbf{t}_3^{1'}\otimes\mathbf{t}_3^{1'}+\mathbf{t}_1^{1'}\otimes\mathbf{t}_1^{1'}\right)+\sin\left(\theta_1\right)\left(\mathbf{t}_1^{1'}\otimes\mathbf{t}_3^{1'}-\mathbf{t}_3^{1'}\otimes\mathbf{t}_1^{1'}\right)+\mathbf{t}_2^{1'}\otimes\mathbf{t}_2^{1'} \quad (2.5)$$

where the intermediate co-rotational basis, $\mathbf{t}_i^{1'}$, is defined as

$$\mathbf{t}_i^{1'}=\mathbf{L}_1\left(\psi_1,\mathbf{E}_i\right)\mathbf{E}_i \quad (2.6)$$

The co-rotational $\mathbf{t}_i^{\alpha}$ is applied to the center-of-mass of the α bearing; an example for bearings 1 and 2 can be seen in Figure 2.3.

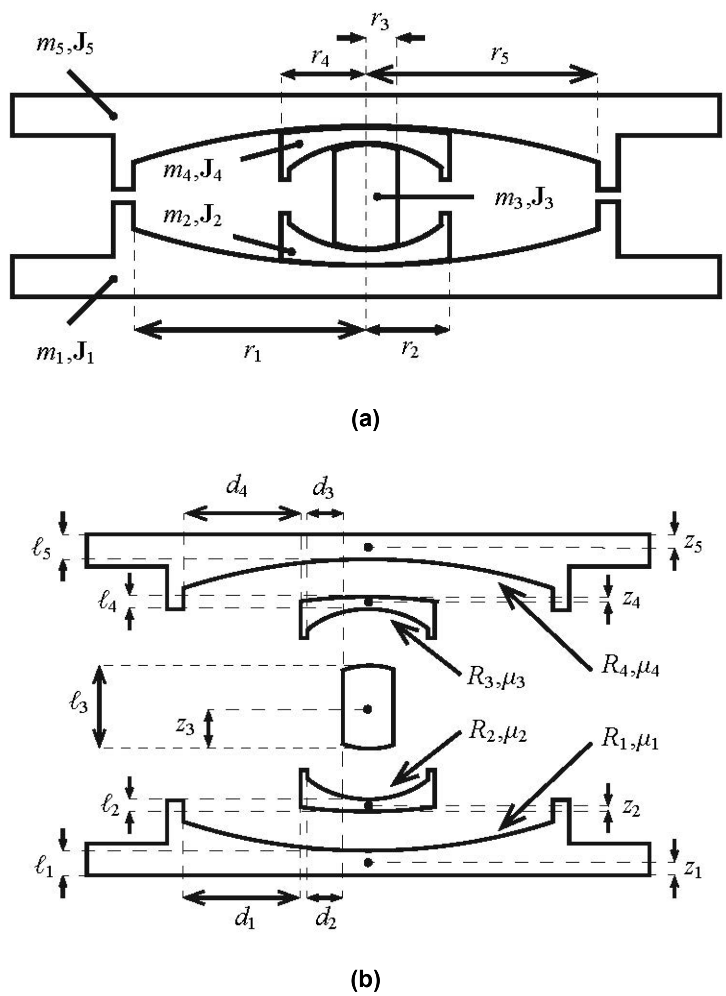

Figure 2.1 (a) Diagram of a Triple Friction Pendulum (TFP) model; and (b) expanded view of the TFP.

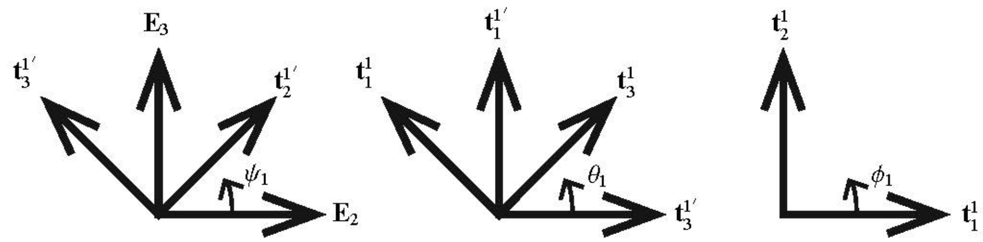

Figure 2.2 **The 2-D change of coordinates from the 1-2-3 Euler angles. Note that in each 2-D coordinate system shown, there is a third unit vector pointing out of the page following the right-hand rule about which the 2-D coordinate system is rotating.**

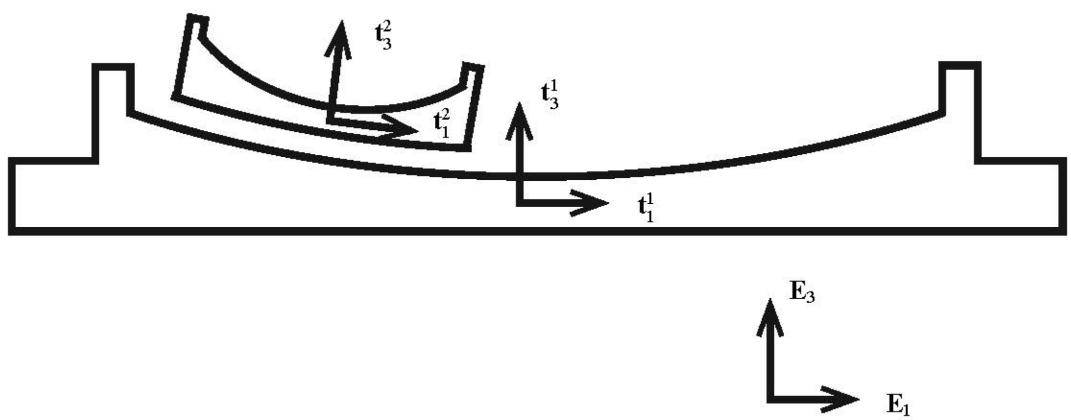

Figure 2.3 **Locations of the co-rotational basis vectors for the first two bearings. Note that for each coordinate system shown, there is a third vector pointing into the page following the right-hand rule.**

The position vectors will all be defined relative to the previous bearing using these co-rotational bases—starting from the ground contact point with the bottom bearing—defined as $\mathbf{r}_{01}$, going all the way to the top of the final bearing, defined as $\mathbf{r}_{55}$. Figures 2.1 and 2.4 show what all of the physical qualities represent, as well as the physical locations of some of the required position vectors.

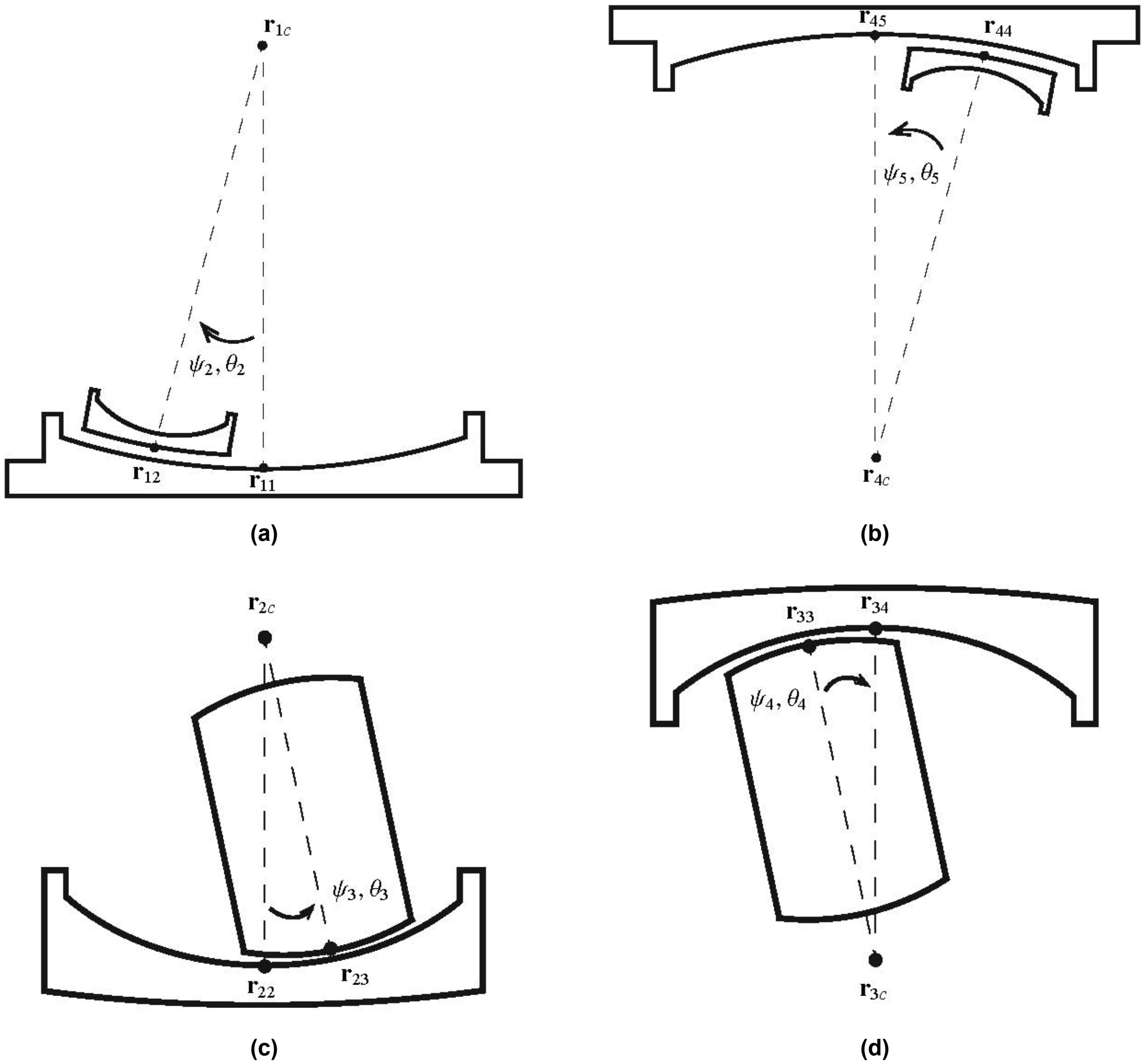

Figure 2.4 Sliding angles for all four sliding surfaces.

All of the required position vectors are defined as follows:

$$\mathbf{r}_{01} = u_{g1}\mathbf{E}_1 + u_{g2}\mathbf{E}_2 + u_{g3}\mathbf{E}_3 \tag{2.7}$$

which is the ground contact point of bearing one,

$$\mathbf{r}_1 = \mathbf{r}_{01} + z_1\mathbf{t}_3^1 \tag{2.8}$$

which is the center-of-mass of bearing one,

$$\mathbf{r}_{11} = \mathbf{r}_1 + \left(\ell_1 - z_1\right)\mathbf{t}_3^1 \tag{2.9}$$

which is the center top of bearing one,

$$\mathbf{r}_{1c} = \mathbf{r}_{11} + R_1\mathbf{t}_3^1 \tag{2.10}$$

which is the center of the sphere created by the sliding surface with radius R_1,

$$\mathbf{r}_{12} = \mathbf{r}_{1c} - R_1 \mathbf{t}_3^1 \tag{2.11}$$

which is the center bottom of bearing two,

$$\mathbf{r}_2 = \mathbf{r}_{12} + z_2 \mathbf{t}_3^2 \tag{2.12}$$

which is the center-of-mass of bearing two,

$$\mathbf{r}_{22} = \mathbf{r}_2 + \left(\ell_2 - z_2\right)\mathbf{t}_3^2 \tag{2.13}$$

which is the center top of bearing two,

$$\mathbf{r}_{2c} = \mathbf{r}_{22} + R_2 \mathbf{t}_3^2 \tag{2.14}$$

which is the center of the sphere created by the sliding surface with radius R_2,

$$\mathbf{r}_{23} = \mathbf{r}_{2c} - R_2 \mathbf{t}_3^3 \tag{2.15}$$

which is the center bottom of bearing three,

$$\mathbf{r}_3 = \mathbf{r}_{23} + z_3 \mathbf{t}_3^3 \tag{2.16}$$

which is the center-of-mass of bearing three,

$$\mathbf{r}_{33} = \mathbf{r}_3 + \left(\ell_3 - z_3\right)\mathbf{t}_3^3 \tag{2.17}$$

which is the center top of bearing three,

$$\mathbf{r}_{3c} = \mathbf{r}_{33} - R_3 \mathbf{t}_3^3 \tag{2.18}$$

which is the center of the sphere created by the sliding surface with radius R_3,

$$\mathbf{r}_{34} = \mathbf{r}_{3c} + R_3 \mathbf{t}_3^4 \tag{2.19}$$

which is the center bottom of bearing four,

$$\mathbf{r}_4 = \mathbf{r}_{34} + \left(\ell_3 - z_4\right)\mathbf{t}_3^4 \tag{2.20}$$

which is the center-of-mass of bearing four,

$$\mathbf{r}_{44} = \mathbf{r}_4 + z_4 \mathbf{t}_3^4 \tag{2.21}$$

which is the center top of bearing four,

$$\mathbf{r}_{4c} = \mathbf{r}_{44} - R_4 \mathbf{t}_3^4 \tag{2.22}$$

which is the center of the sphere created by the sliding surface with radius R_4,

$$\mathbf{r}_{45} = \mathbf{r}_{4c} + R_4 \mathbf{t}_3^5 \tag{2.23}$$

which is the center bottom of bearing five,

$$\mathbf{r}_5 = \mathbf{r}_{45} + \left(\ell_5 - z_5\right)\mathbf{t}_3^5 \tag{2.24}$$

which is the center-of-mass of bearing five,

$$\mathbf{r}_{55} = \mathbf{r}_5 + z_5\mathbf{t}_3^5 \tag{2.25}$$

which is the center top of bearing five,

Now that all of the relevant position vectors have been defined, the velocity vectors associated with each position vector need to be defined. In addition, the angular velocities of each bearing are needed:

$$\boldsymbol{\omega}_1 = \dot{\theta}_1\mathbf{t}_2^1 + \dot{\psi}_1\mathbf{E}_1 \tag{2.26}$$

which is the angular velocity of bearing one excluding any rotational about the axis of symmetry.

$$\boldsymbol{\omega}_1^t = \dot{\phi}_1\mathbf{t}_3^1 + \boldsymbol{\omega}_1 \tag{2.27}$$

which is the total angular velocity of bearing one,

$$\boldsymbol{\omega}_2 = \dot{\theta}_2\mathbf{t}_2^2 + \dot{\psi}_2\mathbf{t}_1^1 + \boldsymbol{\omega}_1 \tag{2.28}$$

which is the angular velocity of bearing two excluding any rotation about the axis of symmetry.

$$\boldsymbol{\omega}_2^t = \dot{\phi}_2\mathbf{t}_3^2 + \boldsymbol{\omega}_2 \tag{2.29}$$

which is the total angular velocity of bearing two

$$\boldsymbol{\omega}_3 = \dot{\theta}_3\mathbf{t}_2^3 + \dot{\psi}_3\mathbf{t}_1^2 + \boldsymbol{\omega}_2 \tag{2.30}$$

which is the total angular velocity of bearing three excluding any rotation about the axis of symmetry,

$$\boldsymbol{\omega}_3^t = \dot{\phi}_3\mathbf{t}_3^3 + \boldsymbol{\omega}_3 \tag{2.31}$$

which is the angular velocity of bearing three,

$$\boldsymbol{\omega}_4 = \dot{\theta}_4\mathbf{t}_2^4 + \dot{\psi}_4\mathbf{t}_1^3 + \boldsymbol{\omega}_3 \tag{2.32}$$

which is the angular velocity of bearing four excluding any rotation about the axis of symmetry,

$$\boldsymbol{\omega}_4^t = \dot{\phi}_4\mathbf{t}_3^4 + \boldsymbol{\omega}_4 \tag{2.33}$$

which is the total angular velocity of bearing four,

$$\boldsymbol{\omega}_5 = \dot{\theta}_5\mathbf{t}_2^5 + \dot{\psi}_5\mathbf{t}_1^4 + \boldsymbol{\omega}_4 \tag{2.34}$$

which is the angular velocity of bearing five excluding any rotation about the axis of symmetry, and

$$\boldsymbol{\omega}_5^t = \dot{\phi}_5\mathbf{t}_3^5 + \boldsymbol{\omega}_5 \tag{2.35}$$

which is the total angular velocity of bearing five. Using the following relations,

$$\dot{\mathbf{t}}_i^1 = \boldsymbol{\omega}_1 \times \mathbf{t}_i^1 \quad \dot{\mathbf{t}}_i^2 = \boldsymbol{\omega}_2 \times \mathbf{t}_i^2 \quad \dot{\mathbf{t}}_i^3 = \boldsymbol{\omega}_3 \times \mathbf{t}_i^3 \quad \dot{\mathbf{t}}_i^4 = \boldsymbol{\omega}_4 \times \mathbf{t}_i^4 \quad \dot{\mathbf{t}}_i^5 = \boldsymbol{\omega}_5 \times \mathbf{t}_i^5 \tag{2.36}$$

the velocity vectors are defined as follows:

$$\mathbf{v}_{01} = \dot{u}_{g1}\mathbf{E}_1 + \dot{u}_{g2}\mathbf{E}_2 + \dot{u}_{g3}\mathbf{E}_3 \quad (2.37)$$

$$\mathbf{v}_1 = \mathbf{v}_{01} + z_1\boldsymbol{\omega}_1 \times \mathbf{t}_3^1 \quad (2.38)$$

$$\mathbf{v}_{11} = \mathbf{v}_1 + z_1\boldsymbol{\omega}_1 \times \mathbf{t}_3^1 \quad (2.39)$$

$$\mathbf{v}_{1c} = \mathbf{v}_{11} + R_1\boldsymbol{\omega}_1 \times \mathbf{t}_3^1 \quad (2.40)$$

$$\mathbf{v}_{12} = \mathbf{v}_{1c} + R_1\boldsymbol{\omega}_1 \times \mathbf{t}_3^1 \quad (2.41)$$

$$\mathbf{v}_2 = \mathbf{v}_{12} + z_2\boldsymbol{\omega}_1 \times \mathbf{t}_3^2 \quad (2.42)$$

$$\mathbf{v}_{22} = \mathbf{v}_2 + \left(\ell_2 - z_2\right)\boldsymbol{\omega}_2 \times \mathbf{t}_3^2 \quad (2.43)$$

$$\mathbf{v}_{2c} = \mathbf{v}_{22} + R_2\boldsymbol{\omega}_2 \times \mathbf{t}_3^2 \quad (2.44)$$

$$\mathbf{v}_{23} = \mathbf{v}_{2c} - R_2\boldsymbol{\omega}_3 \times \mathbf{t}_3^3 \quad (2.45)$$

$$\mathbf{v}_3 = \mathbf{v}_{23} + z_3\boldsymbol{\omega}_3 \times \mathbf{t}_3^3 \quad (2.46)$$

$$\mathbf{v}_{33} = \mathbf{v}_3 + \left(\ell_3 - z_3\right)\boldsymbol{\omega}_3 \times \mathbf{t}_3^3 \quad (2.47)$$

$$\mathbf{v}_{3c} = \mathbf{v}_{33} - R_3\boldsymbol{\omega}_3 \times \mathbf{t}_3^3 \quad (2.48)$$

$$\mathbf{v}_{34} = \mathbf{v}_{3c} + R_3\boldsymbol{\omega}_4 \times \mathbf{t}_3^4 \quad (2.49)$$

$$\mathbf{v}_4 = \mathbf{v}_{34} + \left(\ell_4 - z_4\right)\boldsymbol{\omega}_4 \times \mathbf{t}_3^4 \quad (2.50)$$

$$\mathbf{v}_{44} = \mathbf{v}_4 + z_4\boldsymbol{\omega}_4 \times \mathbf{t}_3^4 \quad (2.51)$$

$$\mathbf{v}_{4c} = \mathbf{v}_{44} - R_4\boldsymbol{\omega}_4 \times \mathbf{t}_3^4 \quad (2.52)$$

$$\mathbf{v}_{45} = \mathbf{v}_{4c} + R_4\boldsymbol{\omega}_4 \times \mathbf{t}_3^4 \quad (2.53)$$

$$\mathbf{v}_5 = \mathbf{v}_{45} + \left(\ell_5 - z_5\right)\boldsymbol{\omega}_5 \times \mathbf{t}_3^5 \quad (2.54)$$

$$\mathbf{v}_{55} = \mathbf{v}_5 + z_5\boldsymbol{\omega}_5 \times \mathbf{t}_3^5 \quad (2.55)$$

where Equations (2.37)–(2.55) are the velocity vectors of the corresponding position vectors in Equations (2.7)–(2.25). Next the following angular acceleration vectors are required:

$$\dot{\boldsymbol{\omega}}_1 = \ddot{\theta}_1\mathbf{t}_2^1 + \boldsymbol{\omega}_1 \times \dot{\theta}_1\mathbf{t}_2^1 + \ddot{\psi}_1\mathbf{E}_1 \quad (2.56)$$

$$\dot{\boldsymbol{\omega}}_1^t = \ddot{\phi}_1\mathbf{t}_3^1 + \boldsymbol{\omega}_1 \times \dot{\phi}_1\mathbf{t}_3^1 + \dot{\boldsymbol{\omega}}_1 \quad (2.57)$$

$$\dot{\boldsymbol{\omega}}_2 = \ddot{\theta}_2\mathbf{t}_2^2 + \boldsymbol{\omega}_2 \times \dot{\theta}_2\mathbf{t}_2^2 + \ddot{\psi}_2\mathbf{t}_1^1 + \boldsymbol{\omega}_1 \times \dot{\psi}_2\mathbf{t}_1^1 + \dot{\boldsymbol{\omega}}_1 \quad (2.58)$$

$$\dot{\boldsymbol{\omega}}_2^t = \ddot{\phi}_2\mathbf{t}_3^2 + \boldsymbol{\omega}_2 \times \dot{\phi}_2\mathbf{t}_3^2 + \dot{\boldsymbol{\omega}}_2 \quad (2.59)$$

$$\dot{\boldsymbol{\omega}}_3 = \ddot{\theta}_3\mathbf{t}_2^3 + \boldsymbol{\omega}_3 \times \dot{\theta}_3\mathbf{t}_2^3 + \ddot{\psi}_3\mathbf{t}_1^2 + \boldsymbol{\omega}_2 \times \dot{\psi}_3\mathbf{t}_1^2 + \dot{\boldsymbol{\omega}}_2 \tag{2.60}$$

$$\dot{\boldsymbol{\omega}}_3^t = \ddot{\phi}_3\mathbf{t}_3^3 + \boldsymbol{\omega}_3 \times \dot{\phi}_3\mathbf{t}_3^3 + \dot{\boldsymbol{\omega}}_3 \tag{2.61}$$

$$\dot{\boldsymbol{\omega}}_4 = \ddot{\theta}_4\mathbf{t}_2^4 + \boldsymbol{\omega}_4 \times \dot{\theta}_4\mathbf{t}_2^4 + \ddot{\psi}_4\mathbf{t}_1^3 + \boldsymbol{\omega}_3 \times \dot{\psi}_4\mathbf{t}_1^3 + \dot{\boldsymbol{\omega}}_3 \tag{2.62}$$

$$\dot{\boldsymbol{\omega}}_4^t = \ddot{\phi}_4\mathbf{t}_3^4 + \boldsymbol{\omega}_4 \times \dot{\phi}_4\mathbf{t}_3^4 + \dot{\boldsymbol{\omega}}_4 \tag{2.63}$$

$$\dot{\boldsymbol{\omega}}_5 = \ddot{\theta}_5\mathbf{t}_2^5 + \boldsymbol{\omega}_5 \times \dot{\theta}_5\mathbf{t}_2^5 + \ddot{\psi}_5\mathbf{t}_1^4 + \boldsymbol{\omega}_4 \times \dot{\psi}_5\mathbf{t}_1^4 + \dot{\boldsymbol{\omega}}_4 \tag{2.64}$$

$$\dot{\boldsymbol{\omega}}_5^t = \ddot{\phi}_5\mathbf{t}_3^5 + \boldsymbol{\omega}_4 \times \dot{\phi}_5\mathbf{t}_3^5 + \dot{\boldsymbol{\omega}}_5 \tag{2.65}$$

where Equations (2.56)–(2.65) are the angular acceleration vectors of the corresponding angular velocity vectors in Equations (2.26)–(2.35). Finally, the acceleration vectors of each of the above listed velocity vectors are defined as follows:

$$\dot{\mathbf{v}}_{01} = \ddot{u}_{g1}\mathbf{E}_1 + \ddot{u}_{g2}\mathbf{E}_2 + \ddot{u}_{g3}\mathbf{E}_3 \tag{2.66}$$

$$\dot{\mathbf{v}}_1 = \dot{\mathbf{v}}_{01} + z_1\dot{\boldsymbol{\omega}}_1 \times \mathbf{t}_3^1 + z_1\boldsymbol{\omega}_1 \times \left(\boldsymbol{\omega}_1 \times \mathbf{t}_3^1\right) \tag{2.67}$$

$$\dot{\mathbf{v}}_{11} = \dot{\mathbf{v}}_1 + \left(\ell_1 - z_1\right)\dot{\boldsymbol{\omega}}_1 \times \mathbf{t}_3^1 + \left(\ell_1 - z_1\right)\boldsymbol{\omega}_1 \times \boldsymbol{\omega}_1 \times \mathbf{t}_3^1 \tag{2.68}$$

$$\dot{\mathbf{v}}_{1c} = \dot{\mathbf{v}}_{11} + R_1\dot{\boldsymbol{\omega}}_1 \times \mathbf{t}_3^1 + R_1\boldsymbol{\omega}_1 \times \left(\boldsymbol{\omega}_1 \times \mathbf{t}_3^1\right) \tag{2.69}$$

$$\dot{\mathbf{v}}_{12} = \dot{\mathbf{v}}_{1c} - R_1\dot{\boldsymbol{\omega}}_2 \times \mathbf{t}_3^2 - R_1\boldsymbol{\omega}_2 \times \left(\boldsymbol{\omega}_2 \times \mathbf{t}_3^2\right) \tag{2.70}$$

$$\dot{\mathbf{v}}_2 = \dot{\mathbf{v}}_{12} + z_2\dot{\boldsymbol{\omega}}_2 \times \mathbf{t}_3^2 + z_2\boldsymbol{\omega}_2 \times \left(\boldsymbol{\omega}_2 \times \mathbf{t}_3^2\right) \tag{2.71}$$

$$\dot{\mathbf{v}}_{22} = \dot{\mathbf{v}}_2 + \left(\ell_2 - z_2\right)\dot{\boldsymbol{\omega}}_2 \times \mathbf{t}_3^2 + \left(\ell_2 - z_2\right)\boldsymbol{\omega}_2 \times \left(\boldsymbol{\omega}_2 \times \mathbf{t}_3^2\right) \tag{2.72}$$

$$\dot{\mathbf{v}}_{2c} = \dot{\mathbf{v}}_{22} + R_2\dot{\boldsymbol{\omega}}_2 \times \mathbf{t}_3^2 + R_2\boldsymbol{\omega}_2 \times \left(\boldsymbol{\omega}_2 \times \mathbf{t}_3^2\right) \tag{2.73}$$

$$\dot{\mathbf{v}}_{23} = \dot{\mathbf{v}}_{2c} - R_2\dot{\boldsymbol{\omega}}_3 \times \mathbf{t}_3^3 - R_2\boldsymbol{\omega}_3 \times \left(\boldsymbol{\omega}_3 \times \mathbf{t}_3^3\right) \tag{2.74}$$

$$\dot{\mathbf{v}}_3 = \dot{\mathbf{v}}_{23} + z_3\dot{\boldsymbol{\omega}}_3 \times \mathbf{t}_3^3 + z_3\boldsymbol{\omega}_3 \times \left(\boldsymbol{\omega}_3 \times \mathbf{t}_3^3\right) \tag{2.75}$$

$$\dot{\mathbf{v}}_{33} = \dot{\mathbf{v}}_3 + \left(\ell_3 - z_3\right)\dot{\boldsymbol{\omega}}_3 \times \mathbf{t}_3^3 + \left(\ell_3 - z_3\right)\boldsymbol{\omega}_3 \times \left(\boldsymbol{\omega}_3 \times \mathbf{t}_3^3\right) \tag{2.76}$$

$$\dot{\mathbf{v}}_{3c} = \dot{\mathbf{v}}_{33} - R_3\dot{\boldsymbol{\omega}}_3 \times \mathbf{t}_3^3 - R_3\boldsymbol{\omega}_3 \times \left(\boldsymbol{\omega}_3 \times \mathbf{t}_3^3\right) \tag{2.77}$$

$$\dot{\mathbf{v}}_{34} = \dot{\mathbf{v}}_{3c} + R_3\dot{\boldsymbol{\omega}}_4 \times \mathbf{t}_3^4 + R_3\boldsymbol{\omega}_4 \times \left(\boldsymbol{\omega}_4 \times \mathbf{t}_3^4\right) \tag{2.78}$$

$$\dot{\mathbf{v}}_4 = \dot{\mathbf{v}}_{34} + \left(\ell_4 - z_4\right)\dot{\boldsymbol{\omega}}_4 \times \mathbf{t}_3^4 + \left(\ell_4 - z_4\right)\boldsymbol{\omega}_4 \times \left(\boldsymbol{\omega}_4 \times \mathbf{t}_3^4\right) \tag{2.79}$$

$$\dot{\mathbf{v}}_{44} = \dot{\mathbf{v}}_4 + z_4\dot{\boldsymbol{\omega}}_4 \times \mathbf{t}_3^4 + z_4\boldsymbol{\omega}_4 \times \left(\boldsymbol{\omega}_4 \times \mathbf{t}_3^4\right) \tag{2.80}$$

$$\dot{\mathbf{v}}_{4c} = \dot{\mathbf{v}}_{44} - R_4\dot{\boldsymbol{\omega}}_4 \times \mathbf{t}_3^4 - R_4\boldsymbol{\omega}_4 \times \left(\boldsymbol{\omega}_4 \times \mathbf{t}_3^4\right) \tag{2.81}$$

$$\dot{\mathbf{v}}_{45} = \dot{\mathbf{v}}_{4c} + R_4\dot{\boldsymbol{\omega}}_5 \times \mathbf{t}_3^5 + R_4\boldsymbol{\omega}_5 \times \left(\boldsymbol{\omega}_5 \times \mathbf{t}_3^5\right) \tag{2.82}$$

$$\dot{\mathbf{v}}_5 = \dot{\mathbf{v}}_{45} + \left(\ell_5 - z_5\right)\dot{\boldsymbol{\omega}}_5 \times \mathbf{t}_3^5 + \left(\ell_5 - z_5\right)\boldsymbol{\omega}_5 \times \left(\boldsymbol{\omega}_5 \times \mathbf{t}_3^5\right) \tag{2.83}$$

$$\dot{\mathbf{v}}_{55} = \dot{\mathbf{v}}_5 + z_5\dot{\boldsymbol{\omega}}_5 \times \mathbf{t}_3^5 + z_5\boldsymbol{\omega}_5 \times \left(\boldsymbol{\omega}_5 \times \mathbf{t}_3^5\right) \tag{2.84}$$

where Equations (2.66)–(2.84) are the acceleration vectors of the corresponding position vectors in Equations (2.7)–(2.25). The following vectors are all of the required vectors to properly describe the kinematics of the TFP.

2.2 NORMAL FORCES

In order to look at the full kinetics of the TFP, all of the forces acting both internally and externally need to be fully des cribbed. The first set of forces that act on the TFP are the internal normal forces. From a moment balance, the normal forces will not necessarily be acting at the center point of the contract between bearings [Sarlis and Constantinou 2016], which requires another set of 1-2 Euler angles to define the location of each internal normal force. These Euler angles and their associated basis vectors shall be noted with a superscribed ~, such as $\tilde{\psi}_1$ and $\tilde{\mathbf{t}}_1^1$. The basis vectors for each normal force position is given as

$$\tilde{\mathbf{t}}_i^1 = \tilde{\mathbf{R}}_1\mathbf{t}_i^1 \quad \tilde{\mathbf{t}}_i^2 = \tilde{\mathbf{R}}_2\mathbf{t}_i^2 \quad \tilde{\mathbf{t}}_i^3 = \tilde{\mathbf{R}}_3\mathbf{t}_i^3 \quad \tilde{\mathbf{t}}_i^4 = \tilde{\mathbf{R}}_4\mathbf{t}_i^4 \quad \tilde{\mathbf{t}}_i^5 = \tilde{\mathbf{R}}_5\mathbf{t}_i^5 \tag{2.85}$$

where

$$\begin{aligned} \tilde{\mathbf{R}}_1 &= \mathbf{R}\left(\tilde{\psi}_1, \tilde{\theta}_1, \mathbf{t}_i^1\right) \quad \tilde{\mathbf{R}}_2 = \mathbf{R}\left(\tilde{\psi}_2, \tilde{\theta}_2, \mathbf{t}_i^2\right) \\ \tilde{\mathbf{R}}_3 &= \mathbf{R}\left(\tilde{\psi}_3, \tilde{\theta}_3, \mathbf{t}_i^3\right) \quad \tilde{\mathbf{R}}_4 = \mathbf{R}\left(\tilde{\psi}_4, \tilde{\theta}_4, \mathbf{t}_i^4\right) \end{aligned} \tag{2.86}$$

where $\mathbf{R}$ has the same definition as in Equation (2.3). The position of each normal force is defined as

$$\tilde{\mathbf{r}}_1 = \mathbf{r}_{1c} - R_1\tilde{\mathbf{t}}_3^1 \tag{2.87}$$

which is the position of the normal force on the sliding surface with radius R_1,

$$\tilde{\mathbf{r}}_2 = \mathbf{r}_{2c} - R_2\tilde{\mathbf{t}}_3^2 \tag{2.88}$$

which is the position of the normal force on the sliding surface with radius R_2,

$$\tilde{\mathbf{r}}_3 = \mathbf{r}_{3c} + R_3\tilde{\mathbf{t}}_3^3 \tag{2.89}$$

which is the position of the normal force on the sliding surface with radius R_3,

$$\tilde{\mathbf{r}}_4 = \mathbf{r}_{4c} + R_4\tilde{\mathbf{t}}_3^4 \tag{2.90}$$

which is the position of the normal force on the sliding surface with radius R_3. Finally, the normal forces are defined as

$$\mathbf{N}_1 = N_1\tilde{\mathbf{t}}_3^1 \quad \mathbf{N}_2 = N_2\tilde{\mathbf{t}}_3^2 \quad \mathbf{N}_3 = N_3\tilde{\mathbf{t}}_3^3 \quad \mathbf{N}_4 = N_4\tilde{\mathbf{t}}_3^4 \tag{2.91}$$

where N_α are the magnitudes of the normal forces. This is all of the required information to define the internal normal forces.

2.3 FRICTION FORCES

The next set of forces acting on the TFP are the friction forces that act between bearings at each of the sliding surfaces. The friction forces act at the same locations as the normal forces, thus they will use the same set of basis vectors and Euler angles previously defined. The dynamic friction forces are in the plane normal to the normal forces and are defined as follows:

$$\mathbf{F}_{f1} = -\mu_1 N_1\tilde{\mathbf{f}}_1 \quad \mathbf{F}_{f2} = -\mu_2 N_2\tilde{\mathbf{f}}_2 \quad \mathbf{F}_{f1} = -\mu_3 N_3\tilde{\mathbf{f}}_3 \quad \mathbf{F}_{f4} = -\mu_4 N_4\tilde{\mathbf{f}}_4 \tag{2.92}$$

where μ_α are the coefficient of frictions for each pair of sliding surfaces, and the $\tilde{\mathbf{f}}_\alpha$ vectors define the direction in which the friction forces act and are given by,

$$\begin{aligned} &\tilde{\mathbf{f}}_1 = Y_1\tilde{\mathbf{t}}_1^1 + Z_1\tilde{\mathbf{t}}_2^1 \quad \tilde{\mathbf{f}}_2 = Y_2\tilde{\mathbf{t}}_1^2 + Z_2\tilde{\mathbf{t}}_2^2 \\ &\tilde{\mathbf{f}}_3 = Y_3\tilde{\mathbf{t}}_1^3 + Z_3\tilde{\mathbf{t}}_2^3 \quad \tilde{\mathbf{f}}_4 = Y_4\tilde{\mathbf{t}}_1^4 + Z_4\tilde{\mathbf{t}}_2^4 \end{aligned} \tag{2.93}$$

where Y_α and Z_α are used to define the direction of the friction forces in the plane normal to the normal forces. These values are determined using a modified Bouc–Wen model for biaxial hysteresis [Park et al. 1986; Harvey and Gavin 2014], given as follows:

$$\begin{aligned} &\dot{Y}_1 = \frac{R_1}{R_0}\left[\left(1-a_1Y_1^2\right)\tilde{u}_1 - b_1Y_1Z_1\tilde{v}_1\right] \quad a_1 = \begin{cases} 1, & Y_1\tilde{u}_1 > 0 \\ 0, & Y_1\tilde{u}_1 \le 0 \end{cases} \\ &\dot{Z}_1 = \frac{R_1}{R_0}\left[\left(1-b_1Z_1^2\right)\tilde{v}_2 - a_1Y_1Z_1\tilde{u}_1\right] \quad b_1 = \begin{cases} 1, & Z_1\tilde{v}_1 > 0 \\ 0, & Z_1\tilde{v}_1 \le 0 \end{cases} \end{aligned} \tag{2.94}$$

$$\begin{aligned} &\dot{Y}_2 = \frac{R_2}{R_0}\left[\left(1-a_2Y_2^2\right)\tilde{u}_2 - b_2Y_2Z_2\tilde{v}_2\right] \quad a_2 = \begin{cases} 1, & Y_2\tilde{u}_2 > 0 \\ 0, & Y_2\tilde{u}_2 \le 0 \end{cases} \\ &\dot{Z}_2 = \frac{R_2}{R_0}\left[\left(1-b_2Z_2^2\right)\tilde{v}_2 - a_2Y_2Z_2\tilde{u}_2\right] \quad b_2 = \begin{cases} 1, & Z_2\tilde{v}_2 > 0 \\ 0, & Z_2\tilde{v}_2 \le 0 \end{cases} \end{aligned} \tag{2.95}$$

$$\begin{aligned} &\dot{Y}_3 = \frac{R_3}{R_0}\left[\left(1-a_3Y_3^2\right)\tilde{u}_3 - b_3Y_3Z_3\tilde{v}_3\right] \quad a_3 = \begin{cases} 1, & Y_3\tilde{u}_3 > 0 \\ 0, & Y_3\tilde{u}_3 \le 0 \end{cases} \\ &\dot{Z}_3 = \frac{R_3}{R_0}\left[\left(1-b_3Z_3^2\right)\tilde{v}_3 - a_3Y_3Z_3\tilde{u}_3\right] \quad b_3 = \begin{cases} 1, & Z_3\tilde{v}_3 > 0 \\ 0, & Z_3\tilde{v}_3 \le 0 \end{cases} \end{aligned} \tag{2.96}$$

$$
\begin{aligned}
\dot{Y}_4 &= \frac{R_4}{R_0}\left[\left(1-a_4Y_4^2\right)\tilde{u}_4 - b_4Y_4Z_4\tilde{v}_4\right] \quad a_4 = \begin{cases} 1, & Y_4\tilde{u}_4 > 0 \\ 0, & Y_4\tilde{u}_4 \le 0 \end{cases} \\
\dot{Z}_4 &= \frac{R_4}{R_0}\left[\left(1-b_4Z_4^2\right)\tilde{v}_4 - a_4Y_4Z_4\tilde{u}_4\right] \quad b_4 = \begin{cases} 1, & Z_4\tilde{v}_4 > 0 \\ 0, & Z_4\tilde{v}_4 \le 0 \end{cases}
\end{aligned} \tag{2.97}
$$

where R_0 is the yield radius, and $\tilde{u}_\alpha$ and $\tilde{v}_\alpha$ are the orthogonal in-plane components of the relative velocity at the point where the friction forces act and are given by

$$
\begin{aligned}
&\tilde{u}_1 = \tilde{\mathbf{v}}_1 \cdot \tilde{\mathbf{t}}_1^1 \quad \tilde{v}_1 = \tilde{\mathbf{v}}_1 \cdot \tilde{\mathbf{t}}_2^1 \quad \tilde{u}_1 = \tilde{\mathbf{v}}_2 \cdot \tilde{\mathbf{t}}_1^2 \quad \tilde{v}_2 = \tilde{\mathbf{v}}_2 \cdot \tilde{\mathbf{t}}_2^2 \\
&\tilde{u}_3 = \tilde{\mathbf{v}}_3 \cdot \tilde{\mathbf{t}}_1^3 \quad \tilde{v}_3 = \tilde{\mathbf{v}}_3 \cdot \tilde{\mathbf{t}}_2^3 \quad \tilde{u}_4 = \tilde{\mathbf{v}}_4 \cdot \tilde{\mathbf{t}}_2^4 \quad \tilde{v}_4 = \tilde{\mathbf{v}}_4 \cdot \tilde{\mathbf{t}}_2^4
\end{aligned} \tag{2.98}
$$

where $\tilde{\mathbf{v}}_\alpha$ are the relative velocity vectors at the points where the friction forces act and are given by

$$
\begin{aligned}
&\tilde{\mathbf{v}}_1 = -R_1\left(\boldsymbol{\omega}_2^t - \boldsymbol{\omega}_1^t\right)\times\tilde{\mathbf{t}}_3^1 \quad \tilde{\mathbf{v}}_2 = -R_2\left(\boldsymbol{\omega}_3^t - \boldsymbol{\omega}_2^t\right)\times\tilde{\mathbf{t}}_3^2 \\
&\tilde{\mathbf{v}}_3 = R_3\left(\boldsymbol{\omega}_4^t - \boldsymbol{\omega}_3^t\right)\times\tilde{\mathbf{t}}_3^3 \qquad \tilde{\mathbf{v}}_4 = R_4\left(\boldsymbol{\omega}_5^t - \boldsymbol{\omega}_4^t\right)\times\tilde{\mathbf{t}}_3^4
\end{aligned} \tag{2.99}
$$

This gives all of the necessary information to fully define the friction forces.

2.4 CONTACT FORCES

The last set of forces acting on the TFP are the forces that occur when two bearings contact one another when the maximum sliding displacement has been reached for a given sliding surface. To model this force, a spring–damper system will be imposed at the contact point. First, the amount of relative sliding between bearings for each sliding surface is given as

$$
\begin{aligned}
&s_1 = R_1\cos^{-1}\left(\mathbf{t}_3^1\cdot\mathbf{t}_3^2\right) \quad s_2 = R_2\cos^{-1}\left(\mathbf{t}_3^2\cdot\mathbf{t}_3^3\right) \\
&s_3 = R_3\cos^{-1}\left(\mathbf{t}_3^3\cdot\mathbf{t}_3^4\right) \quad s_4 = R_4\cos^{-1}\left(\mathbf{t}_3^4\cdot\mathbf{t}_3^5\right)
\end{aligned} \tag{2.100}
$$

The gap functions are then defined as

$$
g_1 = s_{c1} - s_1 \quad g_2 = s_{c2} - s_2 \quad g_3 = s_{c3} - s_3 \quad g_4 = s_{c4} - s_4 \tag{2.101}
$$

where $s_{c\alpha}$ is the maximum sliding displacement before contact. Thus, if g_α is positive, there is no contact; if g_α is negative, there is contact. The velocity gap is defined as

$$
\gamma_1 = \dot{g}_1 \quad \gamma_2 = \dot{g}_2 \quad \gamma_3 = \dot{g}_3 \quad \gamma_4 = \dot{g}_4 \tag{2.102}
$$

The magnitudes of the contact forces become

$$
F_{c1} = \begin{cases} 0 & g_1 > 0 \\ k_{c1}g_1 + c_{c1}\gamma_1 & g_1 \le 0 \end{cases} \tag{2.103}
$$

$$
F_{c2} = \begin{cases} 0 & g_2 > 0 \\ k_{c2}g_2 + c_{c2}\gamma_2 & g_2 \le 0 \end{cases} \tag{2.104}
$$

$$F_{c3}=\begin{cases}0 & g_3>0\\ k_{c3}g_3+c_{c3}\gamma_3 & g_3\le 0\end{cases} \tag{2.105}$$

$$F_{c4}=\begin{cases}0 & g_4>0\\ k_{c4}g_4+c_{c4}\gamma_4 & g_4\le 0\end{cases} \tag{2.106}$$

where $k_{c\alpha}$ and $c_{c\alpha}$ are the stiffness and damping constants for the contact forces, respectively. The contact forces are then given by

$$\mathbf{F}_{c1}=F_{c1}\overline{\mathbf{f}}_1 \quad \mathbf{F}_{c2}=F_{c2}\overline{\mathbf{f}}_2 \quad \mathbf{F}_{c3}=F_{c3}\overline{\mathbf{f}}_3 \quad \mathbf{F}_{c4}=F_{c4}\overline{\mathbf{f}}_4 \tag{2.107}$$

where the directions of the forces are given by

$$\begin{aligned}
\overline{\mathbf{f}}_1&=\frac{\left(\mathbf{t}_3^1\cdot\mathbf{t}_1^2\right)\mathbf{t}_1^2+\left(\mathbf{t}_3^1\cdot\mathbf{t}_2^2\right)\mathbf{t}_2^2}{\sqrt{\left(\mathbf{t}_3^1\cdot\mathbf{t}_1^2\right)^2+\left(\mathbf{t}_3^1\cdot\mathbf{t}_2^2\right)^2}} \quad & \overline{\mathbf{f}}_2&=\frac{\left(\mathbf{t}_3^2\cdot\mathbf{t}_1^3\right)\mathbf{t}_1^3+\left(\mathbf{t}_3^2\cdot\mathbf{t}_2^3\right)\mathbf{t}_2^3}{\sqrt{\left(\mathbf{t}_3^2\cdot\mathbf{t}_1^3\right)^2+\left(\mathbf{t}_3^2\cdot\mathbf{t}_2^3\right)^2}}\\
\overline{\mathbf{f}}_3&=\frac{\left(\mathbf{t}_3^4\cdot\mathbf{t}_1^3\right)\mathbf{t}_1^3+\left(\mathbf{t}_3^4\cdot\mathbf{t}_2^3\right)\mathbf{t}_2^3}{\sqrt{\left(\mathbf{t}_3^4\cdot\mathbf{t}_1^3\right)^2+\left(\mathbf{t}_3^4\cdot\mathbf{t}_2^3\right)^2}} \quad & \overline{\mathbf{f}}_4&=\frac{\left(\mathbf{t}_3^5\cdot\mathbf{t}_1^4\right)\mathbf{t}_1^4+\left(\mathbf{t}_3^5\cdot\mathbf{t}_2^4\right)\mathbf{t}_2^4}{\sqrt{\left(\mathbf{t}_3^5\cdot\mathbf{t}_1^4\right)^2+\left(\mathbf{t}_3^5\cdot\mathbf{t}_2^4\right)^2}}
\end{aligned} \tag{2.108}$$

The contact forces will act at the following positions:

$$\begin{aligned}
\overline{\mathbf{r}}_1&=r_2\overline{\mathbf{f}}_1+p_2\mathbf{t}_3^2+\mathbf{r}_{12} \quad & \overline{\mathbf{r}}_2&=r_3\overline{\mathbf{f}}_2+p_3\mathbf{t}_3^3+\mathbf{r}_{23}\\
\overline{\mathbf{r}}_3&=r_3\overline{\mathbf{f}}_3-p_3\mathbf{t}_3^3+\mathbf{r}_{33} \quad & \overline{\mathbf{r}}_1&=r_4\overline{\mathbf{f}}_4-p_4\mathbf{t}_3^4+\mathbf{r}_{44}
\end{aligned} \tag{2.109}$$

All of the required information needed to define the contact forces between the bearings has been now defined.

2.5 EQUATIONS OF MOTION

Now that all of the required kinematic and kinetic quantities have been defined, the equations of motion for the TFP can be established. In this model, it is assumed that the motion of the base bearing is fully prescribed, meaning u_{g1}, u_{g2}, u_{g3}, ψ_1, θ_1, and ϕ_1, and all required time derivatives are provided. It is also assumed that the force and moment on the top of the bearing—$\mathbf{F}_{\text{top}}$ and $\mathbf{M}_{\text{top}}$–are also provided. From a balance of linear momentum applied to each of the bearings, the following equations much be satisfied:

$$m_2\dot{\mathbf{v}}_2=\mathbf{N}_1+\mathbf{F}_{f1}+\mathbf{F}_{c1}-\mathbf{N}_2-\mathbf{F}_{f2}-\mathbf{F}_{c2}-m_2g\mathbf{E}_3 \tag{2.110}$$

$$m_3\dot{\mathbf{v}}_3=\mathbf{N}_2+\mathbf{F}_{f2}+\mathbf{F}_{c2}-\mathbf{N}_3-\mathbf{F}_{f3}-\mathbf{F}_{c3}-m_3g\mathbf{E}_3 \tag{2.111}$$

$$m_4\dot{\mathbf{v}}_4=\mathbf{N}_3+\mathbf{F}_{f3}+\mathbf{F}_{c3}-\mathbf{N}_4-\mathbf{F}_{f4}-\mathbf{F}_{c4}-m_4g\mathbf{E}_3 \tag{2.112}$$

$$m_5\dot{\mathbf{v}}_5=\mathbf{N}_4+\mathbf{F}_{f4}+\mathbf{F}_{c4}+\mathbf{F}_{\text{top}}-m_5g\mathbf{E}_3 \tag{2.113}$$

where g is the gravitational acceleration, and m_α is the mass of the bearing. Once the balance of angular moment is applied to each bearing, the following equations must also be satisfied:

$$\begin{aligned}\mathbf{J}_2\dot{\boldsymbol{\omega}}_2^t + \boldsymbol{\omega}_2^t \times \mathbf{J}_2\boldsymbol{\omega}_2^t = &\left(\tilde{\mathbf{r}}_1 - \mathbf{r}_2\right)\times\left(\mathbf{N}_1 + \mathbf{F}_{f1}\right) - \left(\tilde{\mathbf{r}}_2 - \mathbf{r}_2\right)\times\left(\mathbf{N}_2 + \mathbf{F}_{f2}\right)\\ &+\left(\overline{\mathbf{r}}_1 - \mathbf{r}_2\right)\times\mathbf{F}_{c1} - \left(\overline{\mathbf{r}}_2 - \mathbf{r}_2\right)\times\mathbf{F}_{c2}\end{aligned} \tag{2.114}$$

$$\begin{aligned}\mathbf{J}_3\dot{\boldsymbol{\omega}}_3^t + \boldsymbol{\omega}_3^t \times \mathbf{J}_3\boldsymbol{\omega}_3^t = &\left(\tilde{\mathbf{r}}_2 - \mathbf{r}_3\right)\times\left(\mathbf{N}_2 + \mathbf{F}_{f2}\right) - \left(\tilde{\mathbf{r}}_3 - \mathbf{r}_3\right)\times\left(\mathbf{N}_3 + \mathbf{F}_{f3}\right)\\ &+\left(\overline{\mathbf{r}}_2 - \mathbf{r}_3\right)\times\mathbf{F}_{c2} - \left(\overline{\mathbf{r}}_3 - \mathbf{r}_3\right)\times\mathbf{F}_{c3}\end{aligned} \tag{2.115}$$

$$\begin{aligned}\mathbf{J}_4\dot{\boldsymbol{\omega}}_4^t + \boldsymbol{\omega}_4^t \times \mathbf{J}_4\boldsymbol{\omega}_4^t = &\left(\tilde{\mathbf{r}}_3 - \mathbf{r}_4\right)\times\left(\mathbf{N}_3 + \mathbf{F}_{f3}\right) - \left(\tilde{\mathbf{r}}_4 - \mathbf{r}_4\right)\times\left(\mathbf{N}_4 + \mathbf{F}_{f4}\right)\\ &+\left(\overline{\mathbf{r}}_3 - \mathbf{r}_4\right)\times\mathbf{F}_{c3} - \left(\overline{\mathbf{r}}_4 - \mathbf{r}_4\right)\times\mathbf{F}_{c4}\end{aligned} \tag{2.116}$$

$$\begin{aligned}\mathbf{J}_5\dot{\boldsymbol{\omega}}_5^t + \boldsymbol{\omega}_5^t \times \mathbf{J}_5\boldsymbol{\omega}_5^t = &\left(\tilde{\mathbf{r}}_4 - \mathbf{r}_5\right)\times\left(\mathbf{N}_4 + \mathbf{F}_{f4}\right) + \left(\overline{\mathbf{r}}_4 - \mathbf{r}_5\right)\times\mathbf{F}_{c4}\\ &+\left(\mathbf{r}_{55} - \mathbf{r}_5\right)\times\mathbf{F}_{\text{top}} + \mathbf{M}_{\text{top}}\end{aligned} \tag{2.117}$$

where $\mathbf{J}_\alpha$ is the mass moment of inertia tensor for each of the bearings and is defined as

$$\mathbf{J}_\alpha = \sum_{i=1}^{3}\lambda_i^\alpha \mathbf{t}_i^\alpha \otimes \mathbf{t}_i^\alpha \tag{2.118}$$

where λ_i^α are the principal moments of inertia of each bearing.

Equations (2.110)–(2.117) provide 24 independent equations for the 24 unknowns, which are

$$\begin{matrix}\ddot{\psi}_2 & \ddot{\theta}_2 & \ddot{\phi}_2 & \ddot{\psi}_3 & \ddot{\theta}_3 & \ddot{\phi}_3 & \ddot{\psi}_4 & \ddot{\theta}_4 & \ddot{\phi}_4 & \ddot{\psi}_5 & \ddot{\theta}_5 & \ddot{\phi}_5\\ \tilde{\psi}_1 & \tilde{\theta}_1 & \tilde{\psi}_2 & \tilde{\theta}_2 & \tilde{\psi}_3 & \tilde{\theta}_3 & \tilde{\psi}_4 & \tilde{\theta}_4 & N_1 & N_2 & N_3 & N_4\end{matrix} \tag{2.119}$$

Note that the equations are nonlinear in the unknowns and must be solved using an iterative solver such as Newton's method. After which, a time integrator such as the Runge–Kutta methods can be used to solve for the time history of the TFP.

3 Expanding to MSFPs

The previous chapter defined the equations of motion for the TFP. Now those equations can be expanded to MSFPs with any number of bearings. Assume one has a MSFP with n bearings, which means there are $n-1$ sliding surfaces., and of those $n-1$ sliding surfaces, m are concave up and $p=n-1-m$ are concave down. Let α be a counting parameter that runs from 1 to m; let β be another counting parameter that runs from $m+1$ to $n-1$; and let γ be a third counting parameter that runs from 1 to $n-1$. Note that for the TFP of the previous chapter, $n=5$, $m=2$, and $p=2$; thus $\alpha=1,2$, $\beta=3,4$, and $\gamma=1,2,3,4$. Using the previous definitions, all of the necessary equations to describe the motion of an MSFP can be written in compact form. The position vectors become

$$\mathbf{r}_{01}=u_{g1}\mathbf{E}_1+u_{g2}\mathbf{E}_2+u_{g3}\mathbf{E}_3 \tag{3.1}$$

$$\mathbf{r}_1=\mathbf{r}_{01}+z_1\mathbf{t}_3^1 \tag{3.2}$$

$$\mathbf{r}_{11}=\mathbf{r}_1+\left(\ell_1-z_1\right)\mathbf{t}_3^1 \tag{3.3}$$

$$\mathbf{r}_{\alpha c}=\mathbf{r}_{\alpha,\alpha}+R_\alpha\mathbf{t}_3^\alpha \tag{3.4}$$

$$\mathbf{r}_{\alpha,\alpha+1}=\mathbf{r}_{\alpha c}-R_\alpha\mathbf{t}_3^{\alpha+1} \tag{3.5}$$

$$\mathbf{r}_{\alpha+1}=\mathbf{r}_{\alpha,\alpha+1}+z_{\alpha+1}\mathbf{t}_3^{\alpha+1} \tag{3.6}$$

$$\mathbf{r}_{\alpha+1,\alpha+1}=\mathbf{r}_{\alpha+1}+\left(\ell_{\alpha+1}-z_{\alpha+1}\right)\mathbf{t}_3^{\alpha+1} \tag{3.7}$$

$$\mathbf{r}_{\beta c}=\mathbf{r}_{\beta,\beta}-R_\beta\mathbf{t}_3^\beta \tag{3.8}$$

$$\mathbf{r}_{\beta,\beta+1}=\mathbf{r}_{\beta c}+R_\beta\mathbf{t}_3^{\beta+1} \tag{3.9}$$

$$\mathbf{r}_{\beta+1}=\mathbf{r}_{\beta,\beta+1}+\left(\ell_{\beta+1}-z_{\beta+1}\right)\mathbf{t}_3^{\beta+1} \tag{3.10}$$

$$\mathbf{r}_{\beta+1,\beta+1}=\mathbf{r}_{\beta+1}+z_{\beta+1}\mathbf{t}_3^{\beta+1} \tag{3.11}$$

where all position vectors here have similar physical representations as those from Equations (2.7)–(2.25). Similar representations exist for the velocity and acceleration vectors. The angular velocity vectors become

$$\boldsymbol{\omega}_1 = \dot{\theta}_1 \mathbf{t}_2^1 + \dot{\psi}_1 \mathbf{E}_1 \quad \boldsymbol{\omega}_1^t = \dot{\phi}_1 \mathbf{t}_2^1 + \boldsymbol{\omega}_1$$
$$\boldsymbol{\omega}_{\gamma+1} = \dot{\theta}_{\gamma+1} \mathbf{t}_2^{\gamma+1} + \dot{\psi}_{\gamma+1} \mathbf{t}_1^{\gamma} + \boldsymbol{\omega}_y \quad \boldsymbol{\omega}_{\gamma+1}^t = \dot{\phi}_{\gamma+1} \mathbf{t}_3^{\gamma+1} + \boldsymbol{\omega}_{\gamma+1} \tag{3.12}$$

where the angular velocity vectors have similar physical meaning as the corresponding vectors from Equations (2.26)–(2.35). Similar representations exist for the angular acceleration vectors. The normal force bases become

$$\tilde{\mathbf{t}}_\gamma^i = \tilde{\mathbf{R}}_\gamma \mathbf{t}_\gamma^i \tag{3.13}$$

with the normal forces acting at the following positions:

$$\tilde{\mathbf{r}}_\alpha = \mathbf{r}_{\alpha c} - R_\alpha \tilde{\mathbf{t}}_3^\alpha \quad \tilde{\mathbf{r}}_\beta = \mathbf{r}_{\beta c} - R_\beta \tilde{\mathbf{t}}_3^\beta \tag{3.14}$$

The normal forces are then given as

$$\tilde{\mathbf{N}}_\gamma = N_\gamma \tilde{\mathbf{t}}_3^\gamma \tag{3.15}$$

Next, the friction forces become

$$\mathbf{F}_{f\gamma} = -\mu_\gamma N_\gamma \tilde{\mathbf{f}}_\gamma \tag{3.16}$$

where the direction of the friction forces comes from

$$\tilde{\mathbf{f}}_\gamma = Y_\gamma \tilde{\mathbf{t}}_1^\gamma + Z_\gamma \tilde{\mathbf{t}}_2^\gamma \tag{3.17}$$

and

$$\dot{Y}_\gamma = \frac{R_\gamma}{R_0}\left[\left(1 - a_\gamma Y_\gamma^2\right)\tilde{u}_\gamma - b_\gamma Y_\gamma Z_\gamma \tilde{v}_\gamma\right] \quad a_\gamma = \begin{cases} 1, & Y_\gamma \tilde{u}_\gamma > 0 \\ 0, & Y_\gamma \tilde{u}_\gamma \le 0 \end{cases}$$
$$\dot{Z}_\gamma = \frac{R_\gamma}{R_0}\left[\left(1 - b_\gamma Z_\gamma^2\right)\tilde{v}_\gamma - a_\gamma Y_\gamma Z_\gamma \tilde{u}_\gamma\right] \quad b_y = \begin{cases} 1, & Z_\gamma \tilde{v}_y > 0 \\ 0, & Z_\gamma \tilde{v}_\gamma \le 0 \end{cases} \tag{3.18}$$

The relative velocity at the point that the friction forces act is then defined as

$$\tilde{\mathbf{v}}_\alpha = -R_\alpha \left(\boldsymbol{\omega}_{\alpha+1}^t - \boldsymbol{\omega}_\alpha^t\right) \times \tilde{\mathbf{t}}_3^\alpha \quad \tilde{\mathbf{v}}_\beta = R_\beta \left(\omega_{\beta+1}^t - \boldsymbol{\omega}_\beta^t\right) \times \tilde{\mathbf{t}}_3^\beta \tag{3.19}$$

The sliding displacements and gap functions for each sliding surface become

$$s_\gamma = R_\gamma \cos^{-1}\left(\mathbf{t}_3^\gamma \cdot \mathbf{t}_3^{\gamma+1}\right) \tag{3.20}$$

and

$$g_\gamma = s_{c\gamma} - s_\gamma \tag{3.21}$$

which makes the contact forces

$$\mathbf{F}_{c\gamma} = F_{c\gamma} \overline{\mathbf{f}}_\gamma \tag{3.22}$$

where the magnitudes of the contact forces are given by

$$F_{c\gamma} = \begin{cases} 0 & g_\gamma > 0 \\ k_{c\gamma} g_\gamma + c_{c\gamma} \gamma_\gamma & g_\gamma \le 0 \end{cases} \tag{3.23}$$

and the directions of the contact forces are given by

$$\overline{\mathbf{f}}_\alpha = \frac{\left(\mathbf{t}_3^\alpha \cdot \mathbf{t}_1^{\alpha+1}\right)\mathbf{t}_1^{\alpha+1} + \left(\mathbf{t}_3^\alpha \cdot \mathbf{t}_2^{\alpha+1}\right)\mathbf{t}_2^{\alpha+1}}{\sqrt{\left(\mathbf{t}_3^\alpha \cdot \mathbf{t}_1^{\alpha+1}\right)^2 + \left(\mathbf{t}_3^\alpha \cdot \mathbf{t}_2^{\alpha+1}\right)^2}} \quad \overline{\mathbf{f}}_\beta \frac{\left(\mathbf{t}_3^{\beta+1} \cdot \mathbf{t}_1^\beta\right)\mathbf{t}_1^\beta + \left(\mathbf{t}_3^{\beta+1} \cdot \mathbf{t}_2^\beta\right)\mathbf{t}_2^\beta}{\sqrt{\left(\mathbf{t}_3^{\beta+1} \cdot \mathbf{t}_1^\beta\right)^2 + \left(\mathbf{t}_3^{\beta+1} \cdot \mathbf{t}_2^\beta\right)^2}} \tag{3.24}$$

The contact forces will act at the following positions:

$$\overline{\mathbf{r}}_\alpha = r_{\alpha+1}\overline{\mathbf{f}}_\alpha + p_{\alpha+1}\mathbf{t}_3^{\alpha+1} + \mathbf{r}_{\alpha,\alpha+1} \quad \overline{\mathbf{r}}_\beta = r_\beta \overline{\mathbf{f}}_\beta - p_\beta \mathbf{t}_3^\beta + \mathbf{r}_{\beta,\beta} \tag{3.25}$$

Finally, the equations of motion become

$$m_{\gamma+1}\dot{\mathbf{v}}_{\gamma+1} = \mathbf{N}_\gamma + \mathbf{F}_{f\gamma} + \mathbf{F}_{c\gamma} - \mathbf{N}_{\gamma+1} - \mathbf{F}_{f\gamma+1} - \mathbf{F}_{c\gamma+1} - m_{\gamma+1} g \mathbf{E}_3 \tag{3.26}$$

and

$$\begin{aligned} \mathbf{J}_{\gamma+1}\dot{\boldsymbol{\omega}}_{\gamma+1}^t + \boldsymbol{\omega}_{\gamma+1}^t \times \mathbf{J}_{\gamma+1}\boldsymbol{\omega}_{\gamma+1}^t &= \left(\tilde{\mathbf{r}}_\gamma - \mathbf{r}_{\gamma+1}\right) \times \left(\mathbf{N}_\gamma + \mathbf{F}_{f\gamma}\right) - \left(\tilde{\mathbf{r}}_{\gamma+1} - \mathbf{r}_{\gamma+1}\right) \times \left(\mathbf{N}_{\gamma+1} + \mathbf{F}_{f\gamma+1}\right) \\ &\quad + \left(\overline{\mathbf{r}}_\gamma - \mathbf{r}_{\gamma+1}\right) \times \mathbf{F}_{c\gamma} - \left(\overline{\mathbf{r}}_{\gamma+1} - \mathbf{r}_{\gamma+1}\right) \times \mathbf{F}_{c\gamma+1} \end{aligned} \tag{3.27}$$

except that the top bearing as a modified set of equations to account for the applied force and moment—$\mathbf{F}_{\text{top}}$ and $\mathbf{M}_{\text{top}}$—on the top bearing, given as

$$m_n \dot{\mathbf{v}}_n = \mathbf{N}_{n-1} + \mathbf{F}_{fn-1} + \mathbf{F}_{cn-1} + \mathbf{F}_{\text{top}} - m_n g \mathbf{E}_3 \tag{3.28}$$

and

$$\begin{aligned} \mathbf{J}_n \dot{\boldsymbol{\omega}}_n^t + \boldsymbol{\omega}_n^t \times \mathbf{J}_n \boldsymbol{\omega}_n^t &= \left(\tilde{\mathbf{r}}_{n-1} - \mathbf{r}_n\right) \times \left(\mathbf{N}_{n-1} + \mathbf{F}_{fn-1}\right) + \left(\overline{\mathbf{r}}_{n-1} - \mathbf{r}_n\right) \times \mathbf{F}_{cn-1} \\ &\quad + \left(\mathbf{r}_{n,n} - \mathbf{r}_n\right) \times \mathbf{F}_{\text{top}} + \mathbf{M}_{\text{top}} \end{aligned} \tag{3.29}$$

Using the above listed definitions, one can readily establish the equations of motion for any basic type of MSFP.

4 Analysis of the Triple Friction Pendulum Model

In order to test the effectiveness of this model for MSFPs, the analysis will focus on the TFP as there are many experimental and theoretical results for that system [Fenz and Constantinou 2008c; Fenz and Constantinou 2008b; Becker and Mahin 2012; and Sarlis and Constantinou 2016]. Due to the nonlinearity of the equations of motion for the TFP– see Equations (2.110)–(2.117)–an iterative solver must be utilized to solve for the unknowns shown in Equation (2.119). Herein, Newton's method is used to solve for the unknowns. Once the system unknowns have been determined, a system of ODEs has to be solved to obtain the time-history of the TFP. The time integrator used for all of the analyses will be the Dormand–Prince method [1980], which is a type of Runge–Kutta ODE solver. All of the physical quantities used for the following analysis can be found in Appendix A. For all the simulations, a ground motion will be prescribed for the bottom bearing and a normal force, a restoring force, and a restoring moment will be applied to the top bearing unless otherwise stated.

4.1 UNI-DIRECTIONAL GROUND MOTIONS

For the uni-directional ground motions, a model based on the one used by Fenz and Constantinou [2008b] will be used for comparisons; all of the physical data can be found in Appendix A.1. For standard models of TFPs–$R_1 = R_4 > R_2 = R_3$, $\mu_2 = \mu_3 < \mu_1 < \mu_4$ – it has been well established that there are five stages to the motion [Fenz and Constantinou 2008c; Fenz and Constantinou 2008b; Becker and Mahin 2012; and Sarlis and Constantinou 2016] when there is a ground motion in only one direction:

- **Stage I**: There is motion only on surfaces 2 and 3.
- **Stage II**: Motion on surface 2 stops and begins on surface 1, thus all motion is on surfaces 1 and 3.
- **Stage III**: Motion on surface 3 stops and begins on surface 4, thus all motion is on surfaces 1 and 4.
- **Stage IV**: The sliding capacity of surface 1 is reached and sliding begins on surface 2, thus all motion is on surfaces 2 and 4.

- **Stage V**: The sliding capacity of surface 4 is reached and sliding begins on surface 3, thus all motion is on surfaces 3 and 4. This stage ends when the sliding capacities of both surfaces 2 and 3 are reached.

By running our kinetic model with a uni-directional motion—$u_{g1} = 0.05t^2 m$ and all other prescribed motions set to zero—and imposing a restoring force and moment on the top bearing, this five-stage behavior is created as shown in Figure 4.1; here, F_{top}/N is the restoring force on the top bearing, F_{top}, normalized to the applied normal force, N. Note that the relative angle between bearings is defined as $\delta_\gamma = \cos^{-1}\left[\cos\left(\psi_{\gamma+1}\right)\cos\left(\theta_{\gamma+1}\right)\right]$.

In order to test the hysteresis in this model, a uni-directional periodic ground motion–ug1 = $u_{g1} = A\cos\left(2\pi ft\right)m$–is applied to the system. The same tests used by Fenz and Constantinou [2008b] will be used in this section, which will allow for a direct comparison of results. Table 4.1 shows the list of tests. The force-displacement curves are shown in Figure 4.2. By comparing them to similar figures in Fenz and Constantinou [2008b; 2008c], it can be seen that the kinetic model has the appropriate hysteresis behavior. Regarding the analytical models developed by Fenz and Constantinou [2008b], they note that their forces on the top bearing when the first and fourth sliding surfaces reach their limits–F_{dr1} and F_{dr4}–underestimate the force recorded from the experiment. The values for u^*, u^{**}, u_{dr1}, u_{dr4}, F_{dr1} and F_{dr4} are shown in Table 4.2, where u^* is the displacement at which the TFP transitions from Stage I to Stage II, u^{**} is the displacement at which the TFP transitions from Stage II to Stage III, u_{dr1} is the displacement at which the TFP transitions from Stage III to Stage IV, u_{dr4} is the displacement at which the TFP transitions from Stage IV to Stage V, F_{dr1} is the force at which the TFP transitions from Stage III to Stage IV, and F_{dr4} is the force at which the TFP transitions from Stage IV to Stage V [Fenz and Constantinou 2008c].

Table 4.1 Tests used for uni-directional ground motions.

Test No.	N (kN)	f (Hz)	A (mm)
1	112	0.10	1.2
2	112	0.04	25
3	112	0.013	75
4	112	0.0088	115
5	112	0.0072	140

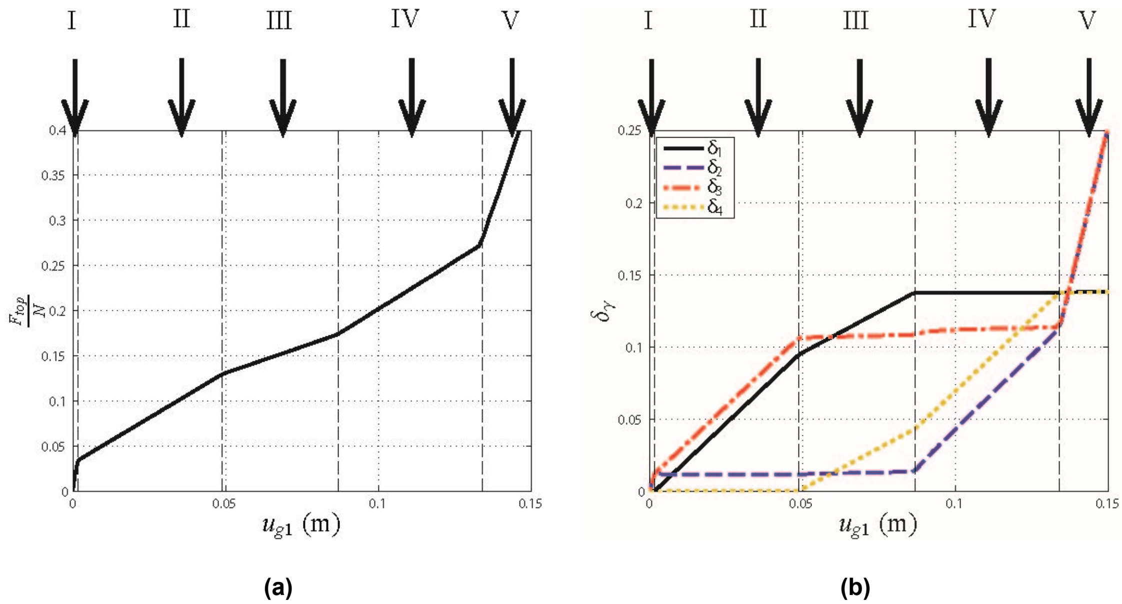

Figure 4.1 **(a) Force/displacement curve for the TFP for a uni-directional motion; and (b) relative angle of each bearing for a uni-directional motion.**

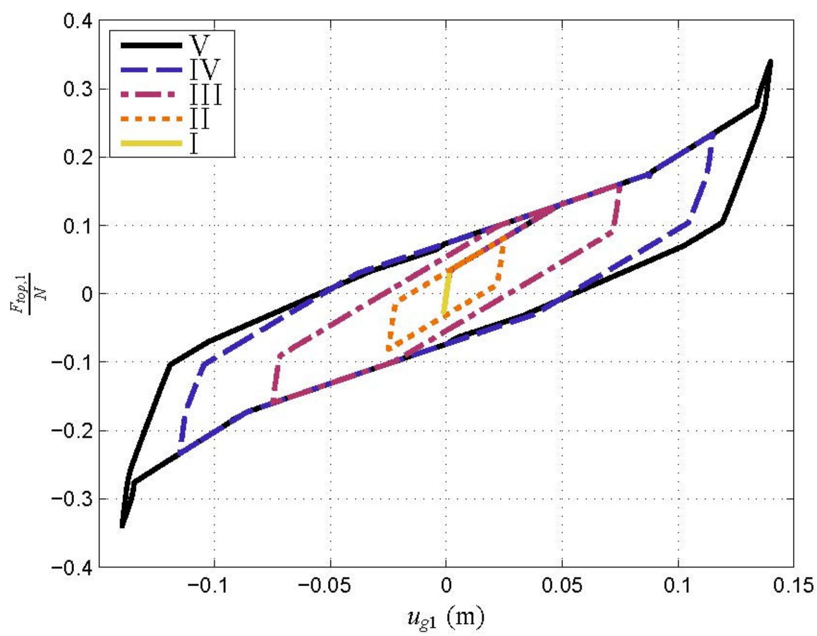

Figure 4.2 **Hysteresis loops for uni-directional motions for ground motions in the five stages of motion.**

Table 4.2 **Comparison of analytical model, experimental, and kinetic model values**

	Analytical†	Experimental†	Kinetic model
u^* (mm)	0.1	2	1.9
u^{**} (mm)	38.4	42	49
u_{dr1} (mm)	92.1	90	87
u_{dr4} (mm)	130.4	130	134
F_{dr1}/N	0.161	0.173	0.175
F_{dr4}/N	0.240	0.272	0.275

† Analytical and experimental values come from the Regime V Data from Fenz and Constantinou (2008b).

From Table 4.2 it can be seen that the kinetic model matches all of these values fairly well. Although the kinetic model slightly overestimates F_{dr1} and F_{dr4}, it is still much closer to the experimental values than the analytical values. The overestimation of F_{dr4} is most likely due to using a constant set of μ_γ values as opposed to changing the friction coefficients with different stages. Thus, it is shown that for larger displacements, the kinetic model more accurately predicts the response of an actual TFP because there is no linearization approximation, which becomes less accurate as the amplitude of motion increases.

For all of the previous tests, a normal force of N = 112 kN was used. However, it is useful to see how changing N affects the dynamic response of the TFP, as this will give a sense of the inertial effects of the model. To do this, the variance between two tests will be measured with an L^2-norm [Johnson 2009] given by

$$V(\eta) = \frac{\sqrt{\int_0^{u_{\max}} \left\| \mathbf{d} - \mathbf{d}_{ref} \right\|^2}}{\sqrt{\int_0^{u_{\max}} \left\| \mathbf{d}_{ref} \right\|^2}} \tag{4.1}$$

where $V(\eta)$ is the variance as a function of η; η is the ratio of the applied normal force to the weight of the TFP, W, excluding the bottom bearing, $u_{\max}$ is the maximum applied ground displacement, and $\mathbf{d}$ is given as

$$\mathbf{d} = \begin{bmatrix} \delta_1 & \delta_2 & \delta_3 & \delta_4 \end{bmatrix}^T \tag{4.2}$$

$\mathbf{d}_{\text{ref}}$ is the test with the largest normal force, $N_{\max}$, to which all other tests will be compared. Herein, $N_{\max}$ = 1 MN, and W = 90.64N. Note that $\left\| \bullet \right\|$ is the standard 2-norm.

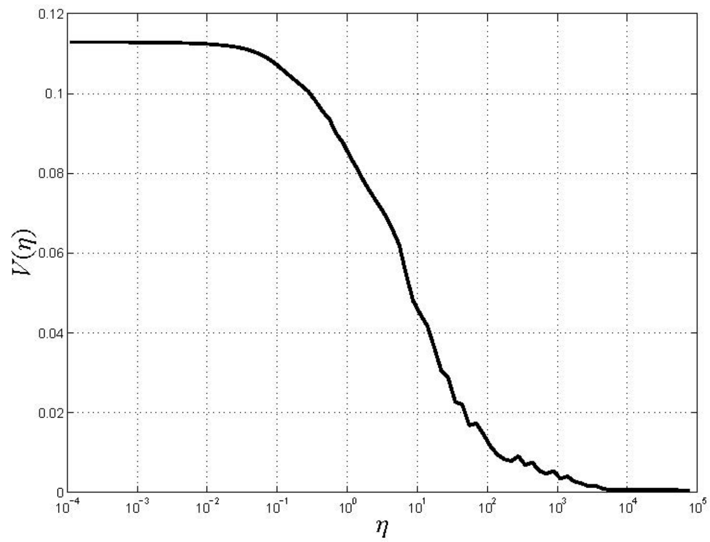

Figure 4.3 The variance between two tests as a function of η on a semi-log scale.

The variance $V(\eta)$ is shown in Figure 4.3, in which it can be seen that the variance is very small for large values of η, but as η decreases, the variance increases until it reaches a plateau around $\eta = 10^{-1}$. Typically values for η will be very large in practice, meaning that the inertial effects can be neglected; however, in the event of uplift [Sarlis and Constantinou 2013], part of the TFP will experience no normal force or $N = \eta = 0$. As can be gleaned from Figure 4.3, in that scenario the inertial effects will play a role.

4.2 UNI-DIRECTIONAL GROUND MOTIONS FOR UNUSUAL TFP PROPERTIES

Another utility of the model presented herein is the lack of assumptions used to develop the model. This allows for new and unique TFPs to be analyzed by this model. For example, the unusual TFP described in Sarlis and Constantinou [2016] has $\mu_2 = \mu_3 > \mu_1 = \mu_4$. While a TFP with this property cannot be analyzed properly by the models presented by Fenz and Constantinou [2008c] or that of Becker and Mahin [2012], it can be analyzed by the nonlinear kinetic model presented herein. Using the same physical properties described in Appendix A.1, except that $\mu_1 = \mu_4 = 0.064$ and $\mu_2 = \mu_3 = 0.168$, the kinetic model can be tested against the results found by Sarlis and Constantinou [2016] by applying a uni-directional ground motion of $u_{g1} = A\cos\left(2\pi ft\right)$, where $A = 0.14m$ and $f = 0.02$ Hz. Figure 4.4 shows the force-displacement curve for the unusual TFP. By comparing Figure 4.4 to similar figures in Sarlis and Constantinou [2016], it can be seen that the kinetic model accurately models the behavior of the unusual TFP.

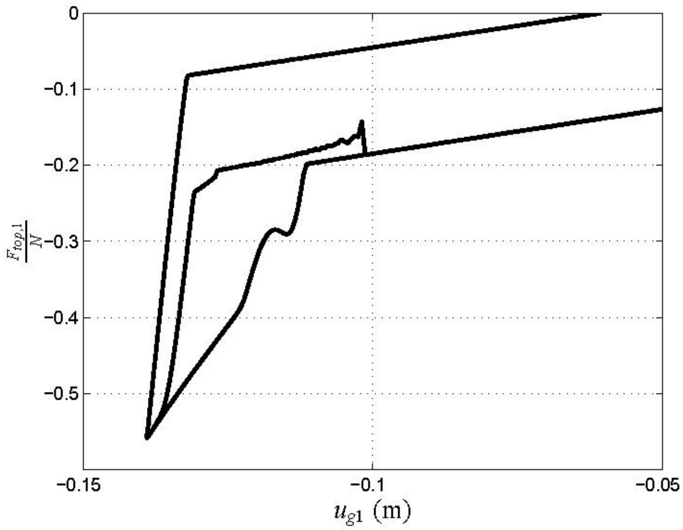

Figure 4.4 Force/displacement curve for the unusual TFP.

4.3 BI-DIRECTIONAL GROUND MOTIONS

Next, the kinetic model is tested with bi-directional ground motions. In the case of bi- directional ground motions, a model based on Becker and Mahin [2012] is used for comparison, and all of the necessary physical data can be found in Appendix A.2. The first test is a circular ground motion: $u_{g1} = A\cos(\Omega t)$ and $u_{g2} = A\sin(\Omega t)$; all of prescribed motions are set to zero. For the circular ground motion tests, Ω = 0.1 rad/sec is used, along with six values for A: A = 0.125, 0.088, 0.050, 0.025, 0.012, 0.005 *m*. This gives a basic ground motion to make sure that the kinetic model has the proper hysteresis loops as the bearings move in two directions. Figure 4.5 shows the hysteresis loops for both the E1 and E2 directions as well as the force curves on the top bearing when a circular ground motion is applied. By comparing these curves to similar ones by Becker and Mahin [2012], also shown in Figure 4.5, it can be seen that the kinetic model is acting appropriately for a simple bi-directional ground motion.

Next, a more complicated ground motion, that of a figure-eight, is applied: $u_{g1} = A\cos(\Omega t)$ and $u_{g2} = A\sin(2\Omega t)$; all other prescribed motions set to zero. Again, Ω = 0.1 is used, along with the same six values of A as for the circular motion: A = 0.125, 0.088, 0.050, 0.025, 0.012, 0.005 *m*. Figure 4.6 shows the hysteresis loops for both the $\mathbf{E}_1$ and $\mathbf{E}_2$ directions as well as the force curves on the top bearing when a figure-eight ground motion is applied. By comparing these curves to similar curves by Becker and Mahin [2012], also shown in Figure 4.6, it can be seen that the kinetic model is accurately predicting the behavior of the TFP for this complicated ground motion.

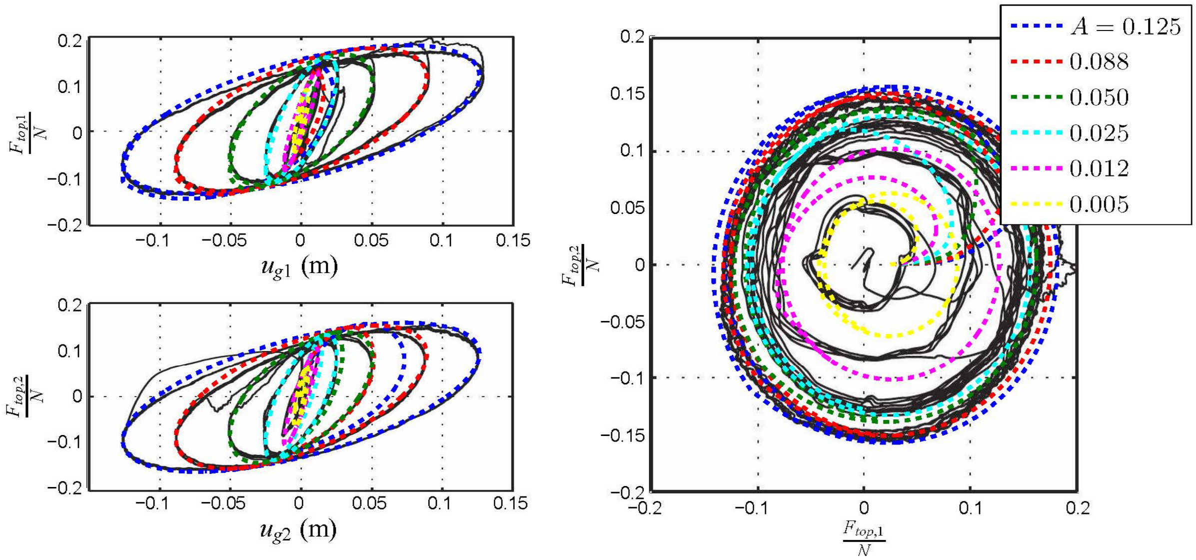

Figure 4.5 **Hysteresis loops and force curves for a circular ground motion. The solid black curves in the background are experimental data from Becker and Mahin [2012].**

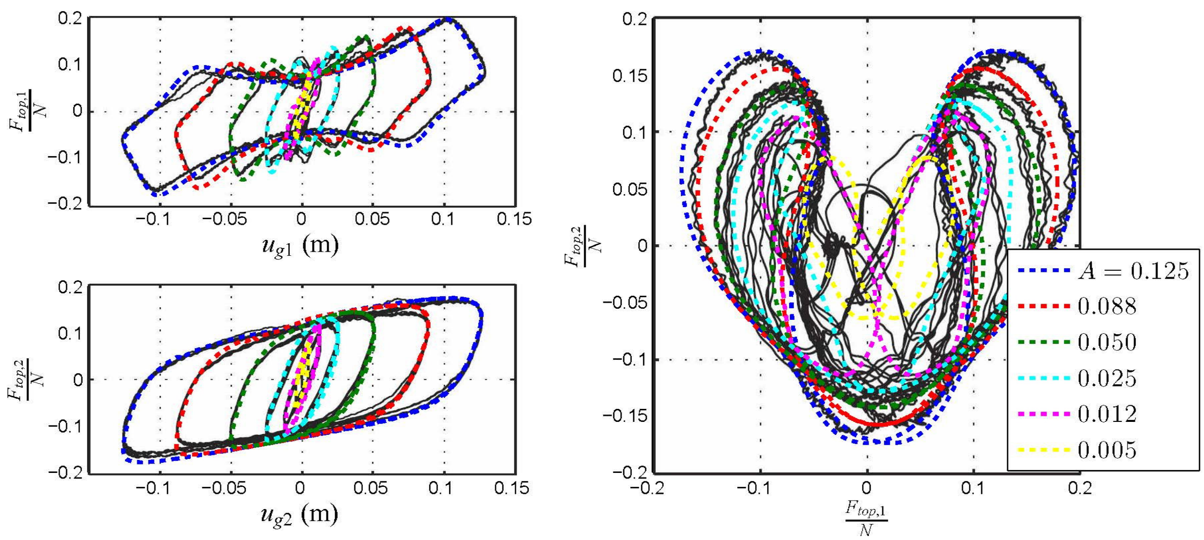

Figure 4.6 **Hysteresis loops and force curves for a figure-eight ground motion. The solid black curves in the background are experimental data from Becker and Mahin [2012].**

5 Conclusions and Future Work

Previously developed kinetic models of triple friction pendulum (TFP) bearings, e.g., Sarlis and Constantinou [2016], linearize the TFP, thereby reducing the accuracy for larger displacements. In addition, they are limited to modeling uni-directional ground motions and are unable to account for the more complicated bi-directional ground motions. Other models account for bi-directional ground motion [Becker and Mahin 2012], but they linearize the model lack the capability to handle non-standard TFP bearings [Sarlis and Constantinou 2013]. The model presented herein accounts for both uni-directional and bi-directional ground motions with no linearization assumption. Thus in the case of uni-directional ground motions, it was shown that the nonlinear model can more accurately predict the experimental values than previous analytical models. The only assumption that our nonlinear kinetic model makes is that the bearings are axisymmetric. Therefore, this model can be used to analyze the simplest as well as the most complicated ground motions. While not specifically analyzed in this paper, the nonlinear kinetic model can account for initial rotations of the top and bottom bearings similar to that described in Becker and Mahin [2013b]. The nonlinear kinetic model has the capability to be connected numerically to models of different superstructures, such as frames, trusses, or any type of finite element model. This allows one to model an entire system, including the TFP in one complete simulation, while accounting for the nonlinear and inertial nature of the TFP.

The model presented herein is not entirely complete: only constant values of the friction coefficients, μ_γ, were used. Kumar et al. [2015] have demonstrated that these values are dependent on multiple factors such as speed, temperature, and pressure; however, implementing these more complicated friction coefficients is a straight forward process that can be added to this model. The nonlinear kinetic model does not account for uplift or tilting of bearings, yet that behavior has been shown to occur in experiments of TFPs [Sarlis and Constantinou 2013]. Our model, however, can be equipped to handle uplift or tilting by adding the necessary degrees-of-freedom to Equation (2.119). It was also shown that the inertial effects of the bearing will have a major role in the event of uplift, thus starting from a model that already incorporates inertia will make handling uplift less complicated. Finally, all of the previous analyses can be conducted with any type of MSFP by the method presented earlier in this paper, allowing for more complicated testing of different types of Friction Pendulum seismic isolators.

For all of the reasons previously stated, the model presented in this paper is an all-in-one model that is the most capable and accurate model for MSFPs available and can be easily updated to handle different types of friction models as well as extra forces that may be applied to the internal bearings.

REFERENCES

Becker T.C., Mahin S.A. (2012). Experimental and analytical study of the bi- directional behavior of the triple friction pendulum isolator, *Earthq. Eng. Struc. Dyn*., 41(3): 355–373.

Becker T.C., Mahin S.A (2013a). Correct treatment of rotation of sliding surfaces in a kinematic model of the triple friction pendulum bearing, *Earthq. Eng. Struc. Dyn*., 42(2) 311–317.

Becker T.C., Mahin S.A. (2013b). Effect of support rotation on triple friction pendulum bearing behavior, *Earthq. Eng. Struc. Dyn*., 42(12): 1731–1748.

Constantinou M.C., Whittaker A.S., Kalpakis I., Warn G. (2007). Performance of seismic isolation hardware under service and seismic loading, *Technical Report MCEER-07-0012*, SUNY Buffalo, Buffalo, NY.

Dormand J.R., Prince P.J. (1980). A family of embedded Runge-Kutta formulae, *J. Comp. Appl. Math*., 6(1): 19–26.

Fadi F., Constantinou M.C. (2010). Evaluation of simplified methods of analysis for structures with triple friction pendulum isolators, *Earthq. Eng. Struc. Dyn*., 39(1) 5–22.

Fenz D.M., Constantinou M.C. (2008a). Modeling triple friction pendulum bearings for response-history analysis, *Earthq. Spectra* 24(4): 1011–1028.

Fenz D.M., Constantinou M.C. (2008b). Spherical sliding isolation bearings with adaptive behavior: Experimental verification, *Earthq. Eng. Struc. Dyn*., 37(2): 185–205.

Fenz D.M., Constantinou M.C. (2008c). Spherical sliding isolation bearings with adaptive behavior: Theory, *Earthq. Eng. Struc. Dyn*., 37(2): 163–183.

Harvey P.S., Gavin H.P. (2014). Truly isotropic biaxial hysteresis with arbitrary knee sharpness, *Earthq. Eng. Struc. Dyn*., 43(13): 2051–2057

Johnson C. (2009). *Numerical Solution of Partial Differential Equations by the Finite Element Method*. Mineola, NY: Dover Publications.

Kumar M., Whittaker A.S., Constantinou M.C. (2015). Characterizing friction in sliding isolation bearings, *Earthq. Eng. Struc. Dyn*., 44(9): 1409–1425.

Mokha A.S., Amin N., Constantinou M.C., Zayas V. (1996). Seismic isolation retrofit of large historic building, ASCE, *J. Struct. Eng*., 122(3) 298–308.

Morgan T.A., Mahin S.A. (2010). Achieving reliable seismic performance enhancement using multi-stage friction pendulum isolators, *Earthq. Eng. Struc. Dyn*., (39)13: 1443–1461.

Mosqueda G., Whittaker A.S., Fenves G.L. (2004). Characterization and modeling of friction pendulum bearings subjected to multiple components of excitation, ASCE, *J. Struct. Eng*., 3: 433–442.

O'Reilly O.M. (2008). *Intermediate Dynamics for Engineers*, New York: Cambridge University Press.

Park Y.J., Wen Y.K., Ang A.H-S. (1986). Random vibration of hysteretic systems under bi-directional ground motions, *Earthq. Eng. Struc. Dyn*., 14(4): 543–557.

Sarlis A.A., Constantinou M.C. (2013). Model of triple friction pendulum isolators for general geometric and frictional parameters and for uplift conditions, *Technical Report MCEER-13-0010*, Multidisciplinary Center for Earthquake Engineering Research, SUNY Buffalo, Buffalo, NY.

Sarlis A.A., Constantinou M.C. (2016). A model of triple friction pendulum bearing for general geometric and frictional parameters, *Earthq. Eng. Struc. Dyn*., 11: 1837–1853.

Tsai C.S., Lin Y.C., Su H.C. (2010). Characterization and modeling of multiple friction pendulum isolation system with numerous sliding interfaces, *Earthq. Eng. Struc. Dyn*., 39(13) 1463–1491.

Warn G.P., Ryan K.L. (2012). A review of seismic isolation for buildings: Historical development and research needs, *Buildings*, 2(3): 300–325.

Zayas V.A., Low S.S. (1999). Seismic isolation of bridges using friction pendulum bearings, Proceedings, *Structural Engineering in the 21st Century: Structures Congress,* ASCE, New Orleans, LA.

Zayas V.A., Low S.S., Mahin S.A. (1987). The FPS earthquake protection system: Experimental report, *Report No. UCB/EERC-1987/01*, Earthquake Engineering Research Center, University of California, Berkeley, CA.

Appendix A Physical Data

The following tables provide all of the numerical values used throughout report, along with g = 9.8 m/sec^2

A.1 UNI-DIRECTIONAL GROUND MOTIONS

All values chosen for uni-directional ground motions were based on the data provided by Fenz and Constantinou [2008a; 2008b] in order to allow for direct comparison of results.

Table A.1 All lengths used for uni-directional ground motions.

R_1	R_2	R_3	R_4	R_0	r_2	r_3	r_4
0.473 m	0.076 m	0.076 m	0.473 m	5×10^{-5} m	0.051 m	0.0255 m	0.051 m
ℓ_1	ℓ_2	ℓ_3	ℓ_4	ℓ_5	p_2	p_3	p_4
0.013 m	0.015 m	0.046 m	0.015 m	0.013 m	0.0028 m	0.0044 m	0.0028 m
z_2	z_3	z_4	z_5	s_{C1}	s_{C2}	s_{C3}	s_{C4}
0.0075 m	0.023 m	0.0075 m	0.0065 m	0.065 m	0.0215 m	0.0215 m	0.065 m

Table A.2 All masses used for uni-directional ground motions.

m_2	m_3	m_4	m_5
0.45 kg	0.34 kg	0.45 kg	8.0 kg

Table A.3 All inertias used for uni-directional ground motions.

$\mathbf{J}_2$	$\mathbf{J}_3$
$\begin{bmatrix} 3.01 & 0 & 0 \\ 0 & 3.01 & 0 \\ 0 & 0 & 5.85 \end{bmatrix}_{\mathbf{t}_i^2 \otimes \mathbf{t}_j^2} \times 10^{-4}\ \mathrm{kg} \cdot m^2$	$\begin{bmatrix} 1.15 & 0 & 0 \\ 0 & 1.15 & 0 \\ 0 & 0 & 1.11 \end{bmatrix}_{\mathbf{t}_i^3 \otimes \mathbf{t}_j^3} \times 10^{-4}\ \mathrm{kg} \cdot m^2$
$\mathbf{J}_4$	$\mathbf{J}_5$
$\begin{bmatrix} 3.01 & 0 & 0 \\ 0 & 3.01 & 0 \\ 0 & 0 & 5.85 \end{bmatrix}_{\mathbf{t}_i^4 \otimes \mathbf{t}_j^4} \times 10^{-4}\ \mathrm{kg} \cdot m^2$	$\begin{bmatrix} 3.14 & 0 & 0 \\ 0 & 3.14 & 0 \\ 0 & 0 & 6.25 \end{bmatrix}_{\mathbf{t}_i^5 \otimes \mathbf{t}_j^5} \times 10^{-2}\ \mathrm{kg} \cdot m^2$

Table A.4 All stiffnesses and damping constants used for uni-directional ground motions.

$k_{c\gamma}$	k_{top}	$c_{c\gamma}$	c_{top}	μ_1	μ_2	μ_3	μ_4
10^7 *N*/m	10^6 N/m	5 *N* sec/m	5 N ·sec/m	0.03	0.017	0.017	0.107

A.2 BI-DIRECTIONONAL GROUND MOTIONS

All values chosen for bi-directional ground motions were based on the data provided by Becker and Mahin [2012] in order to allow for direct comparison of results.

Table A.5 All lengths used for bi-directional ground motions.

R_1	R_2	R_3	R_4	R_0	r_2	r_3	r_4
0.9906 m	0.0762 m	0.0762 m	0.9906 m	5 × 10−5 m	0.0381 m	0.0191 m	0.0381 m
ℓ_1	ℓ_2	ℓ_3	ℓ_4	ℓ_5	p_2	p_3	p_4
0.011 m	0.0127 m	0.0254 m	0.0127 m	0.011 m	0.00073 m	0.0024 m	0.00073 m
z_2	z_3	z_4	z_5	s_{c_1}	s_{c_2}	s_{c_3}	s_{c_4}
0.0063 m	0.0127 m	0.0063 m	0.0055 m	0.0918 m	0.0135 m	0.0135 m	0.0918 m

Table A.6 All masses used for bi-directional ground motions.

m_2	m_3	m_4	m_5
0.45 kg	0.34 kg	0.45 kg	8.0 kg

Table A.7 All inertias used for bi-directional ground motions.

$\mathbf{J}_2$	$\mathbf{J}_3$
$\begin{bmatrix} 1.69 & 0 & 0 \\ 0 & 1.69 & 0 \\ 0 & 0 & 3.27 \end{bmatrix}_{\mathbf{t}_i^2 \otimes \mathbf{t}_j^2} \times 10^{-4}\ \mathrm{kg} \cdot m^2$	$\begin{bmatrix} 4.91 & 0 & 0 \\ 0 & 4.91 & 0 \\ 0 & 0 & 6.17 \end{bmatrix}_{\mathbf{t}_i^3 \otimes \mathbf{t}_j^3} \times 10^{-5}\ \mathrm{kg} \cdot m^2$
$\mathbf{J}_4$	$\mathbf{J}_5$
$\begin{bmatrix} 1.69 & 0 & 0 \\ 0 & 1.69 & 0 \\ 0 & 0 & 3.27 \end{bmatrix}_{\mathbf{t}_i^4 \otimes \mathbf{t}_j^4} \times 10^{-4}\ \mathrm{kg} \cdot m^2$	$\begin{bmatrix} 3.93 & 0 & 0 \\ 0 & 3.93 & 0 \\ 0 & 0 & 7.84 \end{bmatrix}_{\mathbf{t}_i^5 \otimes \mathbf{t}_j^5} \times 10^{-2}\ \mathrm{kg} \cdot m^2$

Table A.8 All stiffnesses and damping constants used for bi-directional ground motions.

$k_{c\gamma}$	k_{top}	$c_{c\gamma}$	c_{top}	μ_1	μ_2	μ_3	μ_4
107 N/m	106 N/m	5 N sec/m	5 N sec/m	0.118	0.036	0.036	0.137

PEER REPORTS

PEER reports are available as a free PDF download from http://peer.berkeley.edu/publications/peer_reports_complete.html. Printed hard copies of PEER reports can be ordered directly from our printer by following the instructions at http://peer.berkeley.edu/publications/peer_reports.html. For other related questions about the PEER Report Series, contact the Pacific Earthquake Engineering Research Center, 325 Davis Hall, Mail Code 1792, Berkeley, CA 94720. Tel.: (510) 642-3437; Fax: (510) 642-1655; Email: peer_center@berkeley.edu.

PEER 2017/06 *Guidelines for Performance-Based Seismic Design of Tall Buildings, Version 2.03*. TBI Working Group led by co-chairs Ron Hamburger and Jack Moehle: Jack Baker, Jonathan Bray, C.B. Crouse, Greg Deierlein, John Hooper, Marshall Lew, Joe Maffei, Stephen Mahin, James Malley, Farzad Naeim, Jonathan Stewart, and John Wallace. May 2017.

PEER 2017/05 *Recommendations for Ergodic Nonlinear Site Amplification in Central and Eastern North America*. Youssef M.A. Hashash, Joseph A. Harmon, Okan Ilhan, Grace A. Parker, and Jonathan P. Stewart. March 2017.

PEER 2017/04 *Expert Panel Recommendations for Ergodic Site Amplification in Central and Eastern North America*. Jonathan P. Stewart, Grace A Parker, Joseph P. Harmon, Gail M. Atkinson, David M. Boore, Robert B. Darragh, Walter J. Silva, and Youssef M.A. Hashash. March 2017.

PEER 2017/03 *NGA-East Ground-Motion Models for the U.S. Geological Survey National Seismic Hazard Maps*. Christine A. Goulet, Yousef Bozorgnia, Nicolas Kuehn, Linda Al Atik, Robert R. Youngs, Robert W. Graves, and Gail M. Atkinson. March 2017.

PEER 2017/02 *U.S.–New Zealand–Japan Workshop: Liquefaction-Induced Ground Movements Effects, University of California, Berkeley, California, 2–4 November 2016.* Jonathan D. Bray, Ross W. Boulanger, Misko Cubrinovski, Kohji Tokimatsu, Steven L. Kramer, Thomas O'Rourke, Ellen Rathje, Russell A. Green, Peter K. Robinson, and Christine Z. Beyzaei. March 2017.

PEER 2017/01 *2016 PEER Annual Report*. Khalid Mosalam, Amarnath Kasalanati, and Grace Kang. March 2017.

PEER 2016/11 *Seismic Design Guidelines for Tall Buildings*. Members of the Committee for the Tall Buildings Initiative. December 2016.

PEER 2016/10 *Performance-Based Robust Nonlinear Seismic Analysis with Application to Reinforced Concrete Bridge Systems*. Xiao Ling and Khalid M. Mosalam. December 2016.

PEER 2016/09 *Resilience of Critical Structures, Infrastructure, and Communities***.** Gian Paolo Cimellaro, Ali Zamani-Noori, Omar Kamouh, Vesna Terzic, and Stephen A. Mahin. December 2016.

PEER 2016/08 *Processing and Development of Iran Earthquake Ground-Motion Database*. Tadahiro Kishida, Sahar Derakhshan, Sifat Muin, Yousef Bozorgnia, Sean K. Ahdi, Jonathan P. Stewart, Robert B. Darragh, Walter J. Silva, and Esmael Farzanegan. December 2016.

PEER 2016/07 *Hybrid Simulation Theory for a Classical Nonlinear Dynamical System*. Paul L. Drazin and Sanjay Govindjee. September 2016.

PEER 2016/06 *California Earthquake Early Warning System Benefit Study*. Laurie A. Johnson, Sharyl Rabinovici, Grace S. Kang, and Stephen A. Mahin. July 2006.

PEER 2016/05 *Ground-Motion Prediction Equations for Arias Intensity Consistent with the NGA-West2 Ground-Motion Models.* Charlotte Abrahamson, Hao-Jun Michael Shi, and Brian Yang. July 2016.

PEER 2016/04 *The M_W 6.0 South Napa Earthquake of August 24, 2014: A Wake-Up Call for Renewed Investment in Seismic Resilience Across California.* Prepared for the California Seismic Safety Commission, Laurie A. Johnson and Stephen A. Mahin. May 2016.

PEER 2016/03 *Simulation Confidence in Tsunami-Driven Overland Flow.* Patrick Lynett. May 2016.

PEER 2016/02 *Semi-Automated Procedure for Windowing time Series and Computing Fourier Amplitude Spectra for the NGA-West2 Database.* Tadahiro Kishida, Olga-Joan Ktenidou, Robert B. Darragh, and Walter J. Silva. May 2016.

PEER 2016/01 *A Methodology for the Estimation of Kappa (κ) from Large Datasets: Example Application to Rock Sites in the NGA-East Database and Implications on Design Motions.* Olga-Joan Ktenidou, Norman A. Abrahamson, Robert B. Darragh, and Walter J. Silva. April 2016.

PEER 2015/13 *Self-Centering Precast Concrete Dual-Steel-Shell Columns for Accelerated Bridge Construction: Seismic Performance, Analysis, and Design*. Gabriele Guerrini, José I. Restrepo, Athanassios Vervelidis, and Milena Massari. December 2015.

PEER 2015/12 *Shear-Flexure Interaction Modeling for Reinforced Concrete Structural Walls and Columns under Reversed Cyclic Loading*. Kristijan Kolozvari, Kutay Orakcal, and John Wallace. December 2015.

PEER 2015/11 *Selection and Scaling of Ground Motions for Nonlinear Response History Analysis of Buildings in Performance-Based Earthquake Engineering*. N. Simon Kwong and Anil K. Chopra. December 2015.

PEER 2015/10 *Structural Behavior of Column-Bent Cap Beam-Box Girder Systems in Reinforced Concrete Bridges Subjected to Gravity and Seismic Loads. Part II: Hybrid Simulation and Post-Test Analysis*. Mohamed A. Moustafa and Khalid M. Mosalam. November 2015.

PEER 2015/09 *Structural Behavior of Column-Bent Cap Beam-Box Girder Systems in Reinforced Concrete Bridges Subjected to Gravity and Seismic Loads. Part I: Pre-Test Analysis and Quasi-Static Experiments*. Mohamed A. Moustafa and Khalid M. Mosalam. September 2015.

PEER 2015/08 *NGA-East: Adjustments to Median Ground-Motion Models for Center and Eastern North America*. August 2015.

PEER 2015/07 *NGA-East: Ground-Motion Standard-Deviation Models for Central and Eastern North America*. Linda Al Atik. June 2015.

PEER 2015/06 *Adjusting Ground-Motion Intensity Measures to a Reference Site for which V_{S30} = 3000 m/sec*. David M. Boore. May 2015.

PEER 2015/05 *Hybrid Simulation of Seismic Isolation Systems Applied to an APR-1400 Nuclear Power Plant.* Andreas H. Schellenberg, Alireza Sarebanha, Matthew J. Schoettler, Gilberto Mosqueda, Gianmario Benzoni, and Stephen A. Mahin. April 2015.

PEER 2015/04 *NGA-East: Median Ground-Motion Models for the Central and Eastern North America Region*. April 2015.

PEER 2015/03 *Single Series Solution for the Rectangular Fiber-Reinforced Elastomeric Isolator Compression Modulus*. James M. Kelly and Niel C. Van Engelen. March 2015.

PEER 2015/02 *A Full-Scale, Single-Column Bridge Bent Tested by Shake-Table Excitation.* Matthew J. Schoettler, José I. Restrepo, Gabriele Guerrini, David E. Duck, and Francesco Carrea. March 2015.

PEER 2015/01 *Concrete Column Blind Prediction Contest 2010: Outcomes and Observations.* Vesna Terzic, Matthew J. Schoettler, José I. Restrepo, and Stephen A Mahin. March 2015.

PEER 2014/20 *Stochastic Modeling and Simulation of Near-Fault Ground Motions for Performance-Based Earthquake Engineering*. Mayssa Dabaghi and Armen Der Kiureghian. December 2014.

PEER 2014/19 *Seismic Response of a Hybrid Fiber-Reinforced Concrete Bridge Column Detailed for Accelerated Bridge Construction*. Wilson Nguyen, William Trono, Marios Panagiotou, and Claudia P. Ostertag. December 2014.

PEER 2014/18 *Three-Dimensional Beam-Truss Model for Reinforced Concrete Walls and Slabs Subjected to Cyclic Static or Dynamic Loading*. Yuan Lu, Marios Panagiotou, and Ioannis Koutromanos. December 2014.

PEER 2014/17 *PEER NGA-East Database.* Christine A. Goulet, Tadahiro Kishida, Timothy D. Ancheta, Chris H. Cramer, Robert B. Darragh, Walter J. Silva, Youssef M.A. Hashash, Joseph Harmon, Jonathan P. Stewart, Katie E. Wooddell, and Robert R. Youngs. October 2014.

PEER 2014/16 *Guidelines for Performing Hazard-Consistent One-Dimensional Ground Response Analysis for Ground Motion Prediction*. Jonathan P. Stewart, Kioumars Afshari, and Youssef M.A. Hashash. October 2014.

PEER 2014/15 *NGA-East Regionalization Report: Comparison of Four Crustal Regions within Central and Eastern North America using Waveform Modeling and 5%-Damped Pseudo-Spectral Acceleration Response*. Jennifer Dreiling, Marius P. Isken, Walter D. Mooney, Martin C. Chapman, and Richard W. Godbee. October 2014.

PEER 2014/14 *Scaling Relations between Seismic Moment and Rupture Area of Earthquakes in Stable Continental Regions*. Paul Somerville. August 2014.

PEER 2014/13 *PEER Preliminary Notes and Observations on the August 24, 2014, South Napa Earthquake*. Grace S. Kang and Stephen A. Mahin, Editors. September 2014.

PEER 2014/12 *Reference-Rock Site Conditions for Central and Eastern North America: Part II – Attenuation (Kappa) Definition*. Kenneth W. Campbell, Youssef M.A. Hashash, Byungmin Kim, Albert R. Kottke, Ellen M. Rathje, Walter J. Silva, and Jonathan P. Stewart. August 2014.

PEER 2014/11 *Reference-Rock Site Conditions for Central and Eastern North America: Part I - Velocity Definition*. Youssef M.A. Hashash, Albert R. Kottke, Jonathan P. Stewart, Kenneth W. Campbell, Byungmin Kim, Ellen M. Rathje, Walter J. Silva, Sissy Nikolaou, and Cheryl Moss. August 2014.

PEER 2014/10 *Evaluation of Collapse and Non-Collapse of Parallel Bridges Affected by Liquefaction and Lateral Spreading*. Benjamin Turner, Scott J. Brandenberg, and Jonathan P. Stewart. August 2014.

PEER 2014/09 *PEER Arizona Strong-Motion Database and GMPEs Evaluation*. Tadahiro Kishida, Robert E. Kayen, Olga-Joan Ktenidou, Walter J. Silva, Robert B. Darragh, and Jennie Watson-Lamprey. June 2014.

PEER 2014/08 *Unbonded Pretensioned Bridge Columns with Rocking Detail*. Jeffrey A. Schaefer, Bryan Kennedy, Marc O. Eberhard, and John F. Stanton. June 2014.

PEER 2014/07 *Northridge 20 Symposium Summary Report: Impacts, Outcomes, and Next Steps*. May 2014.

PEER 2014/06 *Report of the Tenth Planning Meeting of NEES/E-Defense Collaborative Research on Earthquake Engineering*. December 2013.

PEER 2014/05 *Seismic Velocity Site Characterization of Thirty-One Chilean Seismometer Stations by Spectral Analysis of Surface Wave Dispersion*. Robert Kayen, Brad D. Carkin, Skye Corbet, Camilo Pinilla, Allan Ng, Edward Gorbis, and Christine Truong. April 2014.

PEER 2014/04 Effect of Vertical Acceleration on Shear Strength of Reinforced Concrete Columns. Hyerin Lee and Khalid M. Mosalam. April 2014.

PEER 2014/03 *Retest of Thirty-Year-Old Neoprene Isolation Bearings.* James M. Kelly and Niel C. Van Engelen. March 2014.

PEER 2014/02 *Theoretical Development of Hybrid Simulation Applied to Plate Structures.* Ahmed A. Bakhaty, Khalid M. Mosalam, and Sanjay Govindjee. January 2014.

PEER 2014/01 *Performance-Based Seismic Assessment of Skewed Bridges.* Peyman Kaviani, Farzin Zareian, and Ertugrul Taciroglu. January 2014.

PEER 2013/26 *Urban Earthquake Engineerin*g. Proceedings of the U.S.-Iran Seismic Workshop. December 2013.

PEER 2013/25 *Earthquake Engineering for Resilient Communities: 2013 PEER Internship Program Research Report Collection.* Heidi Tremayne (Editor), Stephen A. Mahin (Editor), Jorge Archbold Monterossa, Matt Brosman, Shelly Dean, Katherine deLaveaga, Curtis Fong, Donovan Holder, Rakeeb Khan, Elizabeth Jachens, David Lam, Daniela Martinez Lopez, Mara Minner, Geffen Oren, Julia Pavicic, Melissa Quinonez, Lorena Rodriguez, Sean Salazar, Kelli Slaven, Vivian Steyert, Jenny Taing, and Salvador Tena. December 2013.

PEER 2013/24 *NGA-West2 Ground Motion Prediction Equations for Vertical Ground Motions*. September 2013.

PEER 2013/23 *Coordinated Planning and Preparedness for Fire Following Major Earthquakes*. Charles Scawthorn. November 2013.

PEER 2013/22 *GEM-PEER Task 3 Project: Selection of a Global Set of Ground Motion Prediction Equations.* Jonathan P. Stewart, John Douglas, Mohammad B. Javanbarg, Carola Di Alessandro, Yousef Bozorgnia, Norman A. Abrahamson, David M. Boore, Kenneth W. Campbell, Elise Delavaud, Mustafa Erdik, and Peter J. Stafford. December 2013.

PEER 2013/21 *Seismic Design and Performance of Bridges with Columns on Rocking Foundations*. Grigorios Antonellis and Marios Panagiotou. September 2013.

PEER 2013/20 *Experimental and Analytical Studies on the Seismic Behavior of Conventional and Hybrid Braced Frames*. Jiun-Wei Lai and Stephen A. Mahin. September 2013.

PEER 2013/19 *Toward Resilient Communities: A Performance-Based Engineering Framework for Design and Evaluation of the Built Environment.* Michael William Mieler, Bozidar Stojadinovic, Robert J. Budnitz, Stephen A. Mahin, and Mary C. Comerio. September 2013.

PEER 2013/18 *Identification of Site Parameters that Improve Predictions of Site Amplification*. Ellen M. Rathje and Sara Navidi. July 2013.

PEER 2013/17 *Response Spectrum Analysis of Concrete Gravity Dams Including Dam-Water-Foundation Interaction*. Arnkjell Løkke and Anil K. Chopra. July 2013.

PEER 2013/16 *Effect of Hoop Reinforcement Spacing on the Cyclic Response of Large Reinforced Concrete Special Moment Frame Beams.* Marios Panagiotou, Tea Visnjic, Grigorios Antonellis, Panagiotis Galanis, and Jack P. Moehle. June 2013.

PEER 2013/15 *A Probabilistic Framework to Include the Effects of Near-Fault Directivity in Seismic Hazard Assessment*. Shrey Kumar Shahi, Jack W. Baker. October 2013.

PEER 2013/14 *Hanging-Wall Scaling using Finite-Fault Simulations.* Jennifer L. Donahue and Norman A. Abrahamson. September 2013.

PEER 2013/13 *Semi-Empirical Nonlinear Site Amplification and its Application in NEHRP Site Factors*. Jonathan P. Stewart and Emel Seyhan. November 2013.

PEER 2013/12 *Nonlinear Horizontal Site Response for the NGA-West2 Project.* Ronnie Kamai, Norman A. Abramson, Walter J. Silva. May 2013.

PEER 2013/11 *Epistemic Uncertainty for NGA-West2 Models.* Linda Al Atik and Robert R. Youngs. May 2013.

PEER 2013/10 *NGA-West 2 Models for Ground-Motion Directionality.* Shrey K. Shahi and Jack W. Baker. May 2013.

PEER 2013/09 *Final Report of the NGA-West2 Directivity Working Group.* Paul Spudich, Jeffrey R. Bayless, Jack W. Baker, Brian S.J. Chiou, Badie Rowshandel, Shrey Shahi, and Paul Somerville. May 2013.

PEER 2013/08 *NGA-West2 Model for Estimating Average Horizontal Values of Pseudo-Absolute Spectral Accelerations Generated by Crustal Earthquakes*. I. M. Idriss. May 2013.

PEER 2013/07 *Update of the Chiou and Youngs NGA Ground Motion Model for Average Horizontal Component of Peak Ground Motion and Response Spectra*. Brian Chiou and Robert Youngs. May 2013.

PEER 2013/06 *NGA-West2 Campbell-Bozorgnia Ground Motion Model for the Horizontal Components of PGA, PGV, and 5%-Damped Elastic Pseudo-Acceleration Response Spectra for Periods Ranging from 0.01 to 10 sec.* Kenneth W. Campbell and Yousef Bozorgnia. May 2013.

PEER 2013/05 *NGA-West 2 Equations for Predicting Response Spectral Accelerations for Shallow Crustal Earthquakes*. David M. Boore, Jonathan P. Stewart, Emel Seyhan, and Gail M. Atkinson. May 2013.

PEER 2013/04 *Update of the AS08 Ground-Motion Prediction Equations Based on the NGA-West2 Data Set*. Norman Abrahamson, Walter Silva, and Ronnie Kamai. May 2013.

PEER 2013/03 *PEER NGA-West2 Database.* Timothy D. Ancheta, Robert B. Darragh, Jonathan P. Stewart, Emel Seyhan, Walter J. Silva, Brian S.J. Chiou, Katie E. Wooddell, Robert W. Graves, Albert R. Kottke, David M. Boore, Tadahiro Kishida, and Jennifer L. Donahue. May 2013.

PEER 2013/02 *Hybrid Simulation of the Seismic Response of Squat Reinforced Concrete Shear Walls*. Catherine A. Whyte and Bozidar Stojadinovic. May 2013.

PEER 2013/01 *Housing Recovery in Chile: A Qualitative Mid-program Review*. Mary C. Comerio. February 2013.

PEER 2012/08 *Guidelines for Estimation of Shear Wave Velocity.* Bernard R. Wair, Jason T. DeJong, and Thomas Shantz. December 2012.

PEER 2012/07 *Earthquake Engineering for Resilient Communities: 2012 PEER Internship Program Research Report Collection.* Heidi Tremayne (Editor), Stephen A. Mahin (Editor), Collin Anderson, Dustin Cook, Michael Erceg, Carlos Esparza, Jose Jimenez, Dorian Krausz, Andrew Lo, Stephanie Lopez, Nicole McCurdy, Paul Shipman, Alexander Strum, Eduardo Vega. December 2012.

PEER 2012/06 *Fragilities for Precarious Rocks at Yucca Mountain.* Matthew D. Purvance, Rasool Anooshehpoor, and James N. Brune. December 2012.

PEER 2012/05 *Development of Simplified Analysis Procedure for Piles in Laterally Spreading Layered Soils.* Christopher R. McGann, Pedro Arduino, and Peter Mackenzie–Helnwein. December 2012.

PEER 2012/04 *Unbonded Pre-Tensioned Columns for Bridges in Seismic Regions.* Phillip M. Davis, Todd M. Janes, Marc O. Eberhard, and John F. Stanton. December 2012.

PEER 2012/03 *Experimental and Analytical Studies on Reinforced Concrete Buildings with Seismically Vulnerable Beam-Column Joints*. Sangjoon Park and Khalid M. Mosalam. October 2012.

PEER 2012/02 *Seismic Performance of Reinforced Concrete Bridges Allowed to Uplift during Multi-Directional Excitation*. Andres Oscar Espinoza and Stephen A. Mahin. July 2012.

PEER 2012/01 *Spectral Damping Scaling Factors for Shallow Crustal Earthquakes in Active Tectonic Regions.* Sanaz Rezaeian, Yousef Bozorgnia, I. M. Idriss, Kenneth Campbell, Norman Abrahamson, and Walter Silva. July 2012.

PEER 2011/10 *Earthquake Engineering for Resilient Communities: 2011 PEER Internship Program Research Report Collection*. Heidi Faison and Stephen A. Mahin, Editors. December 2011.

PEER 2011/09 *Calibration of Semi-Stochastic Procedure for Simulating High-Frequency Ground Motions*. Jonathan P. Stewart, Emel Seyhan, and Robert W. Graves. December 2011.

PEER 2011/08 *Water Supply in regard to Fire Following Earthquake*. Charles Scawthorn. November 2011.

PEER 2011/07 *Seismic Risk Management in Urban Areas*. Proceedings of a U.S.-Iran-Turkey Seismic Workshop. September 2011.

PEER 2011/06 *The Use of Base Isolation Systems to Achieve Complex Seismic Performance Objectives*. Troy A. Morgan and Stephen A. Mahin. July 2011.

PEER 2011/05 *Case Studies of the Seismic Performance of Tall Buildings Designed by Alternative Means.* Task 12 Report for the Tall Buildings Initiative. Jack Moehle, Yousef Bozorgnia, Nirmal Jayaram, Pierson Jones, Mohsen Rahnama, Nilesh Shome, Zeynep Tuna, John Wallace, Tony Yang, and Farzin Zareian. July 2011.

PEER 2011/04 *Recommended Design Practice for Pile Foundations in Laterally Spreading Ground.* Scott A. Ashford, Ross W. Boulanger, and Scott J. Brandenberg. June 2011.

PEER 2011/03 *New Ground Motion Selection Procedures and Selected Motions for the PEER Transportation Research Program*. Jack W. Baker, Ting Lin, Shrey K. Shahi, and Nirmal Jayaram. March 2011.

PEER 2011/02 *A Bayesian Network Methodology for Infrastructure Seismic Risk Assessment and Decision Support*. Michelle T. Bensi, Armen Der Kiureghian, and Daniel Straub. March 2011.

PEER 2011/01 *Demand Fragility Surfaces for Bridges in Liquefied and Laterally Spreading Ground.* Scott J. Brandenberg, Jian Zhang, Pirooz Kashighandi, Yili Huo, and Minxing Zhao. March 2011.

PEER 2010/05 *Guidelines for Performance-Based Seismic Design of Tall Buildings.* Developed by the Tall Buildings Initiative. November 2010.

PEER 2010/04 *Application Guide for the Design of Flexible and Rigid Bus Connections between Substation Equipment Subjected to Earthquakes.* Jean-Bernard Dastous and Armen Der Kiureghian. September 2010.

PEER 2010/03 *Shear Wave Velocity as a Statistical Function of Standard Penetration Test Resistance and Vertical Effective Stress at Caltrans Bridge Sites.* Scott J. Brandenberg, Naresh Bellana, and Thomas Shantz. June 2010.

PEER 2010/02 *Stochastic Modeling and Simulation of Ground Motions for Performance-Based Earthquake Engineering.* Sanaz Rezaeian and Armen Der Kiureghian. June 2010.

PEER 2010/01 *Structural Response and Cost Characterization of Bridge Construction Using Seismic Performance Enhancement Strategies.* Ady Aviram, Božidar Stojadinović, Gustavo J. Parra-Montesinos, and Kevin R. Mackie. March 2010.

PEER 2009/03 *The Integration of Experimental and Simulation Data in the Study of Reinforced Concrete Bridge Systems Including Soil-Foundation-Structure Interaction.* Matthew Dryden and Gregory L. Fenves. November 2009.

PEER 2009/02 *Improving Earthquake Mitigation through Innovations and Applications in Seismic Science, Engineering, Communication, and Response*. Proceedings of a U.S.-Iran Seismic Workshop. October 2009.

PEER 2009/01 *Evaluation of Ground Motion Selection and Modification Methods: Predicting Median Interstory Drift Response of Buildings*. Curt B. Haselton, Editor. June 2009.

PEER 2008/10 *Technical Manual for Strata.* Albert R. Kottke and Ellen M. Rathje. February 2009.

PEER 2008/09 *NGA Model for Average Horizontal Component of Peak Ground Motion and Response Spectra.* Brian S.-J. Chiou and Robert R. Youngs. November 2008.

PEER 2008/08 *Toward Earthquake-Resistant Design of Concentrically Braced Steel Structures*. Patxi Uriz and Stephen A. Mahin. November 2008.

PEER 2008/07 *Using OpenSees for Performance-Based Evaluation of Bridges on Liquefiable Soils*. Stephen L. Kramer, Pedro Arduino, and HyungSuk Shin. November 2008.

PEER 2008/06 *Shaking Table Tests and Numerical Investigation of Self-Centering Reinforced Concrete Bridge Columns*. Hyung IL Jeong, Junichi Sakai, and Stephen A. Mahin. September 2008.

PEER 2008/05 *Performance-Based Earthquake Engineering Design Evaluation Procedure for Bridge Foundations Undergoing Liquefaction-Induced Lateral Ground Displacement*. Christian A. Ledezma and Jonathan D. Bray. August 2008.

PEER 2008/04 *Benchmarking of Nonlinear Geotechnical Ground Response Analysis Procedures.* Jonathan P. Stewart, Annie On-Lei Kwok, Youssef M. A. Hashash, Neven Matasovic, Robert Pyke, Zhiliang Wang, and Zhaohui Yang. August 2008.

PEER 2008/03 *Guidelines for Nonlinear Analysis of Bridge Structures in California.* Ady Aviram, Kevin R. Mackie, and Božidar Stojadinović. August 2008.

PEER 2008/02 *Treatment of Uncertainties in Seismic-Risk Analysis of Transportation Systems*. Evangelos Stergiou and Anne S. Kiremidjian. July 2008.

PEER 2008/01 *Seismic Performance Objectives for Tall Buildings.* William T. Holmes, Charles Kircher, William Petak, and Nabih Youssef. August 2008.

PEER 2007/12 *An Assessment to Benchmark the Seismic Performance of a Code-Conforming Reinforced Concrete Moment-Frame Building.* Curt Haselton, Christine A. Goulet, Judith Mitrani-Reiser, James L. Beck, Gregory G. Deierlein, Keith A. Porter, Jonathan P. Stewart, and Ertugrul Taciroglu. August 2008.

PEER 2007/11 *Bar Buckling in Reinforced Concrete Bridge Columns.* Wayne A. Brown, Dawn E. Lehman, and John F. Stanton. February 2008.

PEER 2007/10 *Computational Modeling of Progressive Collapse in Reinforced Concrete Frame Structures*. Mohamed M. Talaat and Khalid M. Mosalam. May 2008.

PEER 2007/09 *Integrated Probabilistic Performance-Based Evaluation of Benchmark Reinforced Concrete Bridges*. Kevin R. Mackie, John-Michael Wong, and Božidar Stojadinović. January 2008.

PEER 2007/08 *Assessing Seismic Collapse Safety of Modern Reinforced Concrete Moment-Frame Buildings*. Curt B. Haselton and Gregory G. Deierlein. February 2008.

PEER 2007/07 *Performance Modeling Strategies for Modern Reinforced Concrete Bridge Columns*. Michael P. Berry and Marc O. Eberhard. April 2008.

PEER 2007/06 *Development of Improved Procedures for Seismic Design of Buried and Partially Buried Structures*. Linda Al Atik and Nicholas Sitar. June 2007.

PEER 2007/05 *Uncertainty and Correlation in Seismic Risk Assessment of Transportation Systems*. Renee G. Lee and Anne S. Kiremidjian. July 2007.

PEER 2007/04 *Numerical Models for Analysis and Performance-Based Design of Shallow Foundations Subjected to Seismic Loading.* Sivapalan Gajan, Tara C. Hutchinson, Bruce L. Kutter, Prishati Raychowdhury, José A. Ugalde, and Jonathan P. Stewart. May 2008.

PEER 2007/03 *Beam-Column Element Model Calibrated for Predicting Flexural Response Leading to Global Collapse of RC Frame Buildings*. Curt B. Haselton, Abbie B. Liel, Sarah Taylor Lange, and Gregory G. Deierlein. May 2008.

PEER 2007/02 *Campbell-Bozorgnia NGA Ground Motion Relations for the Geometric Mean Horizontal Component of Peak and Spectral Ground Motion Parameters*. Kenneth W. Campbell and Yousef Bozorgnia. May 2007.

PEER 2007/01 *Boore-Atkinson NGA Ground Motion Relations for the Geometric Mean Horizontal Component of Peak and Spectral Ground Motion Parameters*. David M. Boore and Gail M. Atkinson. May 2007.

PEER 2006/12 Societal Implications of Performance-Based Earthquake Engineering. Peter J. May. May 2007.

PEER 2006/11 *Probabilistic Seismic Demand Analysis Using Advanced Ground Motion Intensity Measures, Attenuation Relationships, and Near-Fault Effects*. Polsak Tothong and C. Allin Cornell. March 2007.

PEER 2006/10 *Application of the PEER PBEE Methodology to the I-880 Viaduct*. Sashi Kunnath. February 2007.

PEER 2006/09 *Quantifying Economic Losses from Travel Forgone Following a Large Metropolitan Earthquake*. James Moore, Sungbin Cho, Yue Yue Fan, and Stuart Werner. November 2006.

PEER 2006/08 *Vector-Valued Ground Motion Intensity Measures for Probabilistic Seismic Demand Analysis*. Jack W. Baker and C. Allin Cornell. October 2006.

PEER 2006/07 *Analytical Modeling of Reinforced Concrete Walls for Predicting Flexural and Coupled–Shear-Flexural Responses*. Kutay Orakcal, Leonardo M. Massone, and John W. Wallace. October 2006.

PEER 2006/06 *Nonlinear Analysis of a Soil-Drilled Pier System under Static and Dynamic Axial Loading*. Gang Wang and Nicholas Sitar. November 2006.

PEER 2006/05 *Advanced Seismic Assessment Guidelines.* Paolo Bazzurro, C. Allin Cornell, Charles Menun, Maziar Motahari, and Nicolas Luco. September 2006.

PEER 2006/04 *Probabilistic Seismic Evaluation of Reinforced Concrete Structural Components and Systems*. Tae Hyung Lee and Khalid M. Mosalam. August 2006.

PEER 2006/03 *Performance of Lifelines Subjected to Lateral Spreading.* Scott A. Ashford and Teerawut Juirnarongrit. July 2006.

PEER 2006/02 *Pacific Earthquake Engineering Research Center Highway Demonstration Project.* Anne Kiremidjian, James Moore, Yue Yue Fan, Nesrin Basoz, Ozgur Yazali, and Meredith Williams. April 2006.

PEER 2006/01 *Bracing Berkeley. A Guide to Seismic Safety on the UC Berkeley Campus.* Mary C. Comerio, Stephen Tobriner, and Ariane Fehrenkamp. January 2006.

PEER 2005/16 *Seismic Response and Reliability of Electrical Substation Equipment and Systems.* Junho Song, Armen Der Kiureghian, and Jerome L. Sackman. April 2006.

PEER 2005/15 *CPT-Based Probabilistic Assessment of Seismic Soil Liquefaction Initiation.* R. E. S. Moss, R. B. Seed, R. E. Kayen, J. P. Stewart, and A. Der Kiureghian. April 2006.

PEER 2005/14 *Workshop on Modeling of Nonlinear Cyclic Load-Deformation Behavior of Shallow Foundations.* Bruce L. Kutter, Geoffrey Martin, Tara Hutchinson, Chad Harden, Sivapalan Gajan, and Justin Phalen. March 2006.

PEER 2005/13 *Stochastic Characterization and Decision Bases under Time-Dependent Aftershock Risk in Performance-Based Earthquake Engineering*. Gee Liek Yeo and C. Allin Cornell. July 2005.

PEER 2005/12 *PEER Testbed Study on a Laboratory Building: Exercising Seismic Performance Assessment.* Mary C. Comerio, Editor. November 2005.

PEER 2005/11 *Van Nuys Hotel Building Testbed Report: Exercising Seismic Performance Assessment.* Helmut Krawinkler, Editor. October 2005.

PEER 2005/10 *First NEES/E-Defense Workshop on Collapse Simulation of Reinforced Concrete Building Structures.* September 2005.

PEER 2005/09 *Test Applications of Advanced Seismic Assessment Guidelines.* Joe Maffei, Karl Telleen, Danya Mohr, William Holmes, and Yuki Nakayama. August 2006.

PEER 2005/08 *Damage Accumulation in Lightly Confined Reinforced Concrete Bridge Columns.* R. Tyler Ranf, Jared M. Nelson, Zach Price, Marc O. Eberhard, and John F. Stanton. April 2006.

PEER 2005/07 *Experimental and Analytical Studies on the Seismic Response of Freestanding and Anchored Laboratory Equipment.* Dimitrios Konstantinidis and Nicos Makris. January 2005.

PEER 2005/06 *Global Collapse of Frame Structures under Seismic Excitations*. Luis F. Ibarra and Helmut Krawinkler. September 2005.

PEER 2005//05 *Performance Characterization of Bench- and Shelf-Mounted Equipment.* Samit Ray Chaudhuri and Tara C. Hutchinson. May 2006.

PEER 2005/04 *Numerical Modeling of the Nonlinear Cyclic Response of Shallow Foundations.* Chad Harden, Tara Hutchinson, Geoffrey R. Martin, and Bruce L. Kutter. August 2005.

PEER 2005/03 *A Taxonomy of Building Components for Performance-Based Earthquake Engineering.* Keith A. Porter. September 2005.

PEER 2005/02 *Fragility Basis for California Highway Overpass Bridge Seismic Decision Making*. Kevin R. Mackie and Božidar Stojadinović. June 2005.

PEER 2005/01 *Empirical Characterization of Site Conditions on Strong Ground Motion.* Jonathan P. Stewart, Yoojoong Choi, and Robert W. Graves. June 2005.

PEER 2004/09 *Electrical Substation Equipment Interaction: Experimental Rigid Conductor Studies.* Christopher Stearns and André Filiatrault. February 2005.

PEER 2004/08 *Seismic Qualification and Fragility Testing of Line Break 550-kV Disconnect Switches.* Shakhzod M. Takhirov, Gregory L. Fenves, and Eric Fujisaki. January 2005.

PEER 2004/07 *Ground Motions for Earthquake Simulator Qualification of Electrical Substation Equipment.* Shakhzod M. Takhirov, Gregory L. Fenves, Eric Fujisaki, and Don Clyde. January 2005.

PEER 2004/06 *Performance-Based Regulation and Regulatory Regimes.* Peter J. May and Chris Koski. September 2004.

PEER 2004/05 *Performance-Based Seismic Design Concepts and Implementation: Proceedings of an International Workshop.* Peter Fajfar and Helmut Krawinkler, Editors. September 2004.

PEER 2004/04 *Seismic Performance of an Instrumented Tilt-up Wall Building.* James C. Anderson and Vitelmo V. Bertero. July 2004.

PEER 2004/03 *Evaluation and Application of Concrete Tilt-up Assessment Methodologies.* Timothy Graf and James O. Malley. October 2004.

PEER 2004/02 *Analytical Investigations of New Methods for Reducing Residual Displacements of Reinforced Concrete Bridge Columns.* Junichi Sakai and Stephen A. Mahin. August 2004.

PEER 2004/01 *Seismic Performance of Masonry Buildings and Design Implications.* Kerri Anne Taeko Tokoro, James C. Anderson, and Vitelmo V. Bertero. February 2004.

PEER 2003/18 *Performance Models for Flexural Damage in Reinforced Concrete Columns.* Michael Berry and Marc Eberhard. August 2003.

PEER 2003/17 *Predicting Earthquake Damage in Older Reinforced Concrete Beam-Column Joints.* Catherine Pagni and Laura Lowes. October 2004.

PEER 2003/16 *Seismic Demands for Performance-Based Design of Bridges.* Kevin Mackie and Božidar Stojadinović. August 2003.

PEER 2003/15 *Seismic Demands for Nondeteriorating Frame Structures and Their Dependence on Ground Motions.* Ricardo Antonio Medina and Helmut Krawinkler. May 2004.

PEER 2003/14 *Finite Element Reliability and Sensitivity Methods for Performance-Based Earthquake Engineering*. Terje Haukaas and Armen Der Kiureghian. April 2004.

PEER 2003/13 *Effects of Connection Hysteretic Degradation on the Seismic Behavior of Steel Moment-Resisting Frames.* Janise E. Rodgers and Stephen A. Mahin. March 2004.

PEER 2003/12 *Implementation Manual for the Seismic Protection of Laboratory Contents: Format and Case Studies*. William T. Holmes and Mary C. Comerio. October 2003.

PEER 2003/11 *Fifth U.S.-Japan Workshop on Performance-Based Earthquake Engineering Methodology for Reinforced Concrete Building Structures*. February 2004.

PEER 2003/10 *A Beam-Column Joint Model for Simulating the Earthquake Response of Reinforced Concrete Frames.* Laura N. Lowes, Nilanjan Mitra, and Arash Altoontash. February 2004.

PEER 2003/09 *Sequencing Repairs after an Earthquake: An Economic Approach.* Marco Casari and Simon J. Wilkie. April 2004.

PEER 2003/08 *A Technical Framework for Probability-Based Demand and Capacity Factor Design (DCFD) Seismic Formats*. Fatemeh Jalayer and C. Allin Cornell. November 2003.

PEER 2003/07 *Uncertainty Specification and Propagation for Loss Estimation Using FOSM Methods.* Jack W. Baker and C. Allin Cornell. September 2003.

PEER 2003/06 *Performance of Circular Reinforced Concrete Bridge Columns under Bidirectional Earthquake Loading*. Mahmoud M. Hachem, Stephen A. Mahin, and Jack P. Moehle. February 2003.

PEER 2003/05 *Response Assessment for Building-Specific Loss Estimation.* Eduardo Miranda and Shahram Taghavi. September 2003.

PEER 2003/04 *Experimental Assessment of Columns with Short Lap Splices Subjected to Cyclic Loads*. Murat Melek, John W. Wallace, and Joel Conte. April 2003.

PEER 2003/03 *Probabilistic Response Assessment for Building-Specific Loss Estimation*. Eduardo Miranda and Hesameddin Aslani. September 2003.

PEER 2003/02 *Software Framework for Collaborative Development of Nonlinear Dynamic Analysis Program*. Jun Peng and Kincho H. Law. September 2003.

PEER 2003/01 *Shake Table Tests and Analytical Studies on the Gravity Load Collapse of Reinforced Concrete Frames.* Kenneth John Elwood and Jack P. Moehle. November 2003.

PEER 2002/24 *Performance of Beam to Column Bridge Joints Subjected to a Large Velocity Pulse.* Natalie Gibson, André Filiatrault, and Scott A. Ashford. April 2002.

PEER 2002/23 *Effects of Large Velocity Pulses on Reinforced Concrete Bridge Columns.* Greg L. Orozco and Scott A. Ashford. April 2002.

PEER 2002/22 *Characterization of Large Velocity Pulses for Laboratory Testing.* Kenneth E. Cox and Scott A. Ashford. April 2002.

PEER 2002/21 *Fourth U.S.-Japan Workshop on Performance-Based Earthquake Engineering Methodology for Reinforced Concrete Building Structures*. December 2002.

PEER 2002/20 *Barriers to Adoption and Implementation of PBEE Innovations.* Peter J. May. August 2002.

PEER 2002/19 *Economic-Engineered Integrated Models for Earthquakes: Socioeconomic Impacts.* Peter Gordon, James E. Moore II, and Harry W. Richardson. July 2002.

PEER 2002/18 *Assessment of Reinforced Concrete Building Exterior Joints with Substandard Details.* Chris P. Pantelides, Jon Hansen, Justin Nadauld, and Lawrence D. Reaveley. May 2002.

PEER 2002/17 *Structural Characterization and Seismic Response Analysis of a Highway Overcrossing Equipped with Elastomeric Bearings and Fluid Dampers: A Case Study*. Nicos Makris and Jian Zhang. November 2002.

PEER 2002/16 *Estimation of Uncertainty in Geotechnical Properties for Performance-Based Earthquake Engineering.* Allen L. Jones, Steven L. Kramer, and Pedro Arduino. December 2002.

PEER 2002/15 *Seismic Behavior of Bridge Columns Subjected to Various Loading Patterns*. Asadollah Esmaeily-Gh. and Yan Xiao. December 2002.

PEER 2002/14 *Inelastic Seismic Response of Extended Pile Shaft Supported Bridge Structures.* T.C. Hutchinson, R.W. Boulanger, Y.H. Chai, and I.M. Idriss. December 2002.

PEER 2002/13 *Probabilistic Models and Fragility Estimates for Bridge Components and Systems.* Paolo Gardoni, Armen Der Kiureghian, and Khalid M. Mosalam. June 2002.

PEER 2002/12 *Effects of Fault Dip and Slip Rake on Near-Source Ground Motions: Why Chi-Chi Was a Relatively Mild M7.6 Earthquake*. Brad T. Aagaard, John F. Hall, and Thomas H. Heaton. December 2002.

PEER 2002/11 *Analytical and Experimental Study of Fiber-Reinforced Strip Isolators*. James M. Kelly and Shakhzod M. Takhirov. September 2002.

PEER 2002/10 *Centrifuge Modeling of Settlement and Lateral Spreading with Comparisons to Numerical Analyses***.** Sivapalan Gajan and Bruce L. Kutter. January 2003.

PEER 2002/09 *Documentation and Analysis of Field Case Histories of Seismic Compression during the 1994 Northridge, California, Earthquake*. Jonathan P. Stewart, Patrick M. Smith, Daniel H. Whang, and Jonathan D. Bray. October 2002.

PEER 2002/08 *Component Testing, Stability Analysis and Characterization of Buckling-Restrained Unbonded Braces^{TM}*. Cameron Black, Nicos Makris, and Ian Aiken. September 2002.

PEER 2002/07 *Seismic Performance of Pile-Wharf Connections.* Charles W. Roeder, Robert Graff, Jennifer Soderstrom, and Jun Han Yoo. December 2001.

PEER 2002/06 *The Use of Benefit-Cost Analysis for Evaluation of Performance-Based Earthquake Engineering Decisions*. Richard O. Zerbe and Anthony Falit-Baiamonte. September 2001.

PEER 2002/05 *Guidelines, Specifications, and Seismic Performance Characterization of Nonstructural Building Components and Equipment*. André Filiatrault, Constantin Christopoulos, and Christopher Stearns. September 2001.

PEER 2002/04 *Consortium of Organizations for Strong-Motion Observation Systems and the Pacific Earthquake Engineering Research Center Lifelines Program: Invited Workshop on Archiving and Web Dissemination of Geotechnical Data, 4–5 October 2001*. September 2002.

PEER 2002/03 *Investigation of Sensitivity of Building Loss Estimates to Major Uncertain Variables for the Van Nuys Testbed*. Keith A. Porter, James L. Beck, and Rustem V. Shaikhutdinov. August 2002.

PEER 2002/02 *The Third U.S.-Japan Workshop on Performance-Based Earthquake Engineering Methodology for Reinforced Concrete Building Structures*. July 2002.

PEER 2002/01 *Nonstructural Loss Estimation: The UC Berkeley Case Study.* Mary C. Comerio and John C. Stallmeyer. December 2001.

PEER 2001/16 *Statistics of SDF-System Estimate of Roof Displacement for Pushover Analysis of Buildings.* Anil K. Chopra, Rakesh K. Goel, and Chatpan Chintanapakdee. December 2001.

PEER 2001/15 *Damage to Bridges during the 2001 Nisqually Earthquake.* R. Tyler Ranf, Marc O. Eberhard, and Michael P. Berry. November 2001.

PEER 2001/14 *Rocking Response of Equipment Anchored to a Base Foundation.* Nicos Makris and Cameron J. Black. September 2001.

PEER 2001/13 *Modeling Soil Liquefaction Hazards for Performance-Based Earthquake Engineering*. Steven L. Kramer and Ahmed-W. Elgamal. February 2001.

PEER 2001/12 *Development of Geotechnical Capabilities in OpenSees*. Boris Jeremić. September 2001.

PEER 2001/11 *Analytical and Experimental Study of Fiber-Reinforced Elastomeric Isolators*. James M. Kelly and Shakhzod M. Takhirov. September 2001.

PEER 2001/10 *Amplification Factors for Spectral Acceleration in Active Regions.* Jonathan P. Stewart, Andrew H. Liu, Yoojoong Choi, and Mehmet B. Baturay. December 2001.

PEER 2001/09 *Ground Motion Evaluation Procedures for Performance-Based Design.* Jonathan P. Stewart, Shyh-Jeng Chiou, Jonathan D. Bray, Robert W. Graves, Paul G. Somerville, and Norman A. Abrahamson. September 2001.

PEER 2001/08 *Experimental and Computational Evaluation of Reinforced Concrete Bridge Beam-Column Connections for Seismic Performance*. Clay J. Naito, Jack P. Moehle, and Khalid M. Mosalam. November 2001.

PEER 2001/07 *The Rocking Spectrum and the Shortcomings of Design Guidelines.* Nicos Makris and Dimitrios Konstantinidis. August 2001.

PEER 2001/06 *Development of an Electrical Substation Equipment Performance Database for Evaluation of Equipment Fragilities*. Thalia Agnanos. April 1999.

PEER 2001/05 *Stiffness Analysis of Fiber-Reinforced Elastomeric Isolators.* Hsiang-Chuan Tsai and James M. Kelly. May 2001.

PEER 2001/04 *Organizational and Societal Considerations for Performance-Based Earthquake Engineering*. Peter J. May. April 2001.

PEER 2001/03 *A Modal Pushover Analysis Procedure to Estimate Seismic Demands for Buildings: Theory and Preliminary Evaluation*. Anil K. Chopra and Rakesh K. Goel. January 2001.

PEER 2001/02 *Seismic Response Analysis of Highway Overcrossings Including Soil-Structure Interaction*. Jian Zhang and Nicos Makris. March 2001.

PEER 2001/01 *Experimental Study of Large Seismic Steel Beam-to-Column Connections.* Egor P. Popov and Shakhzod M. Takhirov. November 2000.

PEER 2000/10 *The Second U.S.-Japan Workshop on Performance-Based Earthquake Engineering Methodology for Reinforced Concrete Building Structures*. March 2000.

PEER 2000/09 *Structural Engineering Reconnaissance of the August 17, 1999 Earthquake: Kocaeli (Izmit), Turkey.* Halil Sezen, Kenneth J. Elwood, Andrew S. Whittaker, Khalid Mosalam, John J. Wallace, and John F. Stanton. December 2000.

PEER 2000/08 *Behavior of Reinforced Concrete Bridge Columns Having Varying Aspect Ratios and Varying Lengths of Confinement*. Anthony J. Calderone, Dawn E. Lehman, and Jack P. Moehle. January 2001.

PEER 2000/07 *Cover-Plate and Flange-Plate Reinforced Steel Moment-Resisting Connections.* Taejin Kim, Andrew S. Whittaker, Amir S. Gilani, Vitelmo V. Bertero, and Shakhzod M. Takhirov. September 2000.

PEER 2000/06 *Seismic Evaluation and Analysis of 230-kV Disconnect Switches.* Amir S. J. Gilani, Andrew S. Whittaker, Gregory L. Fenves, Chun-Hao Chen, Henry Ho, and Eric Fujisaki. July 2000.

PEER 2000/05 *Performance-Based Evaluation of Exterior Reinforced Concrete Building Joints for Seismic Excitation*. Chandra Clyde, Chris P. Pantelides, and Lawrence D. Reaveley. July 2000.

PEER 2000/04 *An Evaluation of Seismic Energy Demand: An Attenuation Approach*. Chung-Che Chou and Chia-Ming Uang. July 1999.

PEER 2000/03 *Framing Earthquake Retrofitting Decisions: The Case of Hillside Homes in Los Angeles.* Detlof von Winterfeldt, Nels Roselund, and Alicia Kitsuse. March 2000.

PEER 2000/02 *U.S.-Japan Workshop on the Effects of Near-Field Earthquake Shaking*. Andrew Whittaker, Editor. July 2000.

PEER 2000/01 *Further Studies on Seismic Interaction in Interconnected Electrical Substation Equipment.* Armen Der Kiureghian, Kee-Jeung Hong, and Jerome L. Sackman. November 1999.

PEER 1999/14 *Seismic Evaluation and Retrofit of 230-kV Porcelain Transformer Bushings*. Amir S. Gilani, Andrew S. Whittaker, Gregory L. Fenves, and Eric Fujisaki. December 1999.

PEER 1999/13 *Building Vulnerability Studies: Modeling and Evaluation of Tilt-up and Steel Reinforced Concrete Buildings*. John W. Wallace, Jonathan P. Stewart, and Andrew S. Whittaker, Editors. December 1999.

PEER 1999/12 *Rehabilitation of Nonductile RC Frame Building Using Encasement Plates and Energy-Dissipating Devices*. Mehrdad Sasani, Vitelmo V. Bertero, James C. Anderson. December 1999.

PEER 1999/11 *Performance Evaluation Database for Concrete Bridge Components and Systems under Simulated Seismic Loads*. Yael D. Hose and Frieder Seible. November 1999.

PEER 1999/10 *U.S.-Japan Workshop on Performance-Based Earthquake Engineering Methodology for Reinforced Concrete Building Structures*. December 1999.

PEER 1999/09 *Performance Improvement of Long Period Building Structures Subjected to Severe Pulse-Type Ground Motions*. James C. Anderson, Vitelmo V. Bertero, and Raul Bertero. October 1999.

PEER 1999/08 *Envelopes for Seismic Response Vectors.* Charles Menun and Armen Der Kiureghian. July 1999.

PEER 1999/07 *Documentation of Strengths and Weaknesses of Current Computer Analysis Methods for Seismic Performance of Reinforced Concrete Members*. William F. Cofer. November 1999.

PEER 1999/06 *Rocking Response and Overturning of Anchored Equipment under Seismic Excitations*. Nicos Makris and Jian Zhang. November 1999.

PEER 1999/05 *Seismic Evaluation of 550 kV Porcelain Transformer Bushings.* Amir S. Gilani, Andrew S. Whittaker, Gregory L. Fenves, and Eric Fujisaki. October 1999.

PEER 1999/04 *Adoption and Enforcement of Earthquake Risk-Reduction Measures.* Peter J. May, Raymond J. Burby, T. Jens Feeley, and Robert Wood. August 1999.

PEER 1999/03 *Task 3 Characterization of Site Response General Site Categories*. Adrian Rodriguez-Marek, Jonathan D. Bray and Norman Abrahamson. February 1999.

PEER 1999/02 *Capacity-Demand-Diagram Methods for Estimating Seismic Deformation of Inelastic Structures: SDF Systems*. Anil K. Chopra and Rakesh Goel. April 1999.

PEER 1999/01 *Interaction in Interconnected Electrical Substation Equipment Subjected to Earthquake Ground Motions*. Armen Der Kiureghian, Jerome L. Sackman, and Kee-Jeung Hong. February 1999.

PEER 1998/08 *Behavior and Failure Analysis of a Multiple-Frame Highway Bridge in the 1994 Northridge Earthquake*. Gregory L. Fenves and Michael Ellery. December 1998.

PEER 1998/07 *Empirical Evaluation of Inertial Soil-Structure Interaction Effects.* Jonathan P. Stewart, Raymond B. Seed, and Gregory L. Fenves. November 1998.

PEER 1998/06 *Effect of Damping Mechanisms on the Response of Seismic Isolated Structures*. Nicos Makris and Shih-Po Chang. November 1998.

PEER 1998/05 *Rocking Response and Overturning of Equipment under Horizontal Pulse-Type Motions*. Nicos Makris and Yiannis Roussos. October 1998.

PEER 1998/04 *Pacific Earthquake Engineering Research Invitational Workshop Proceedings, May 14–15, 1998: Defining the Links between Planning, Policy Analysis, Economics and Earthquake Engineering*. Mary Comerio and Peter Gordon. September 1998.

PEER 1998/03 *Repair/Upgrade Procedures for Welded Beam to Column Connections*. James C. Anderson and Xiaojing Duan. May 1998.

PEER 1998/02 *Seismic Evaluation of 196 kV Porcelain Transformer Bushings.* Amir S. Gilani, Juan W. Chavez, Gregory L. Fenves, and Andrew S. Whittaker. May 1998.

PEER 1998/01 *Seismic Performance of Well-Confined Concrete Bridge Columns.* Dawn E. Lehman and Jack P. Moehle. December 2000.

ONLINE PEER REPORTS

The following PEER reports are available by Internet only at http://peer.berkeley.edu/publications/peer_reports_complete.html.

PEER 2012/103 *Performance-Based Seismic Demand Assessment of Concentrically Braced Steel Frame Buildings.* Chui-Hsin Chen and Stephen A. Mahin. December 2012.

PEER 2012/102 *Procedure to Restart an Interrupted Hybrid Simulation: Addendum to PEER Report 2010/103.* Vesna Terzic and Bozidar Stojadinovic. October 2012.

PEER 2012/101 *Mechanics of Fiber Reinforced Bearings.* James M. Kelly and Andrea Calabrese. February 2012.

PEER 2011/107 *Nonlinear Site Response and Seismic Compression at Vertical Array Strongly Shaken by 2007 Niigata-ken Chuetsu-oki Earthquake.* Eric Yee, Jonathan P. Stewart, and Kohji Tokimatsu. December 2011.

PEER 2011/106 *Self Compacting Hybrid Fiber Reinforced Concrete Composites for Bridge Columns.* Pardeep Kumar, Gabriel Jen, William Trono, Marios Panagiotou, and Claudia Ostertag. September 2011.

PEER 2011/105 *Stochastic Dynamic Analysis of Bridges Subjected to Spacially Varying Ground Motions.* Katerina Konakli and Armen Der Kiureghian. August 2011.

PEER 2011/104 *Design and Instrumentation of the 2010 E-Defense Four-Story Reinforced Concrete and Post-Tensioned Concrete Buildings.* Takuya Nagae, Kenichi Tahara, Taizo Matsumori, Hitoshi Shiohara, Toshimi Kabeyasawa, Susumu Kono, Minehiro Nishiyama (Japanese Research Team) and John Wallace, Wassim Ghannoum, Jack Moehle, Richard Sause, Wesley Keller, Zeynep Tuna (U.S. Research Team). June 2011.

PEER 2011/103 *In-Situ Monitoring of the Force Output of Fluid Dampers: Experimental Investigation.* Dimitrios Konstantinidis, James M. Kelly, and Nicos Makris. April 2011.

PEER 2011/102 *Ground-Motion Prediction Equations 1964–2010.* John Douglas. April 2011.

PEER 2011/101 *Report of the Eighth Planning Meeting of NEES/E-Defense Collaborative Research on Earthquake Engineering.* Convened by the Hyogo Earthquake Engineering Research Center (NIED), NEES Consortium, Inc. February 2011.

PEER 2010/111 *Modeling and Acceptance Criteria for Seismic Design and Analysis of Tall Buildings.* Task 7 Report for the Tall Buildings Initiative - Published jointly by the Applied Technology Council. October 2010.

PEER 2010/110 *Seismic Performance Assessment and Probabilistic Repair Cost Analysis of Precast Concrete Cladding Systems for Multistory Buildlings.* Jeffrey P. Hunt and Božidar Stojadinovic. November 2010.

PEER 2010/109 *Report of the Seventh Joint Planning Meeting of NEES/E-Defense Collaboration on Earthquake Engineering. Held at the E-Defense, Miki, and Shin-Kobe, Japan, September 18–19, 2009.* August 2010.

PEER 2010/108 *Probabilistic Tsunami Hazard in California.* Hong Kie Thio, Paul Somerville, and Jascha Polet, preparers. October 2010.

PEER 2010/107 *Performance and Reliability of Exposed Column Base Plate Connections for Steel Moment-Resisting Frames.* Ady Aviram, Božidar Stojadinovic, and Armen Der Kiureghian. August 2010.

PEER 2010/106 *Verification of Probabilistic Seismic Hazard Analysis Computer Programs.* Patricia Thomas, Ivan Wong, and Norman Abrahamson. May 2010.

PEER 2010/105 *Structural Engineering Reconnaissance of the April 6, 2009, Abruzzo, Italy, Earthquake, and Lessons Learned.* M. Selim Günay and Khalid M. Mosalam. April 2010.

PEER 2010/104 *Simulating the Inelastic Seismic Behavior of Steel Braced Frames, Including the Effects of Low-Cycle Fatigue.* Yuli Huang and Stephen A. Mahin. April 2010.

PEER 2010/103 *Post-Earthquake Traffic Capacity of Modern Bridges in California.* Vesna Terzic and Božidar Stojadinović. March 2010.

PEER 2010/102 *Analysis of Cumulative Absolute Velocity (CAV) and JMA Instrumental Seismic Intensity (I_{JMA}) Using the PEER–NGA Strong Motion Database.* Kenneth W. Campbell and Yousef Bozorgnia. February 2010.

PEER 2010/101 *Rocking Response of Bridges on Shallow Foundations.* Jose A. Ugalde, Bruce L. Kutter, and Boris Jeremic. April 2010.

PEER 2009/109 *Simulation and Performance-Based Earthquake Engineering Assessment of Self-Centering Post-Tensioned Concrete Bridge Systems.* Won K. Lee and Sarah L. Billington. December 2009.

PEER 2009/108 *PEER Lifelines Geotechnical Virtual Data Center.* J. Carl Stepp, Daniel J. Ponti, Loren L. Turner, Jennifer N. Swift, Sean Devlin, Yang Zhu, Jean Benoit, and John Bobbitt. September 2009.

PEER 2009/107 *Experimental and Computational Evaluation of Current and Innovative In-Span Hinge Details in Reinforced Concrete Box-Girder Bridges: Part 2: Post-Test Analysis and Design Recommendations.* Matias A. Hube and Khalid M. Mosalam. December 2009.

PEER 2009/106 *Shear Strength Models of Exterior Beam-Column Joints without Transverse Reinforcement.* Sangjoon Park and Khalid M. Mosalam. November 2009.

PEER 2009/105 *Reduced Uncertainty of Ground Motion Prediction Equations through Bayesian Variance Analysis.* Robb Eric S. Moss. November 2009.

PEER 2009/104 *Advanced Implementation of Hybrid Simulation.* Andreas H. Schellenberg, Stephen A. Mahin, Gregory L. Fenves. November 2009.

PEER 2009/103 *Performance Evaluation of Innovative Steel Braced Frames.* T. Y. Yang, Jack P. Moehle, and Božidar Stojadinovic. August 2009.

PEER 2009/102 *Reinvestigation of Liquefaction and Nonliquefaction Case Histories from the 1976 Tangshan Earthquake.* Robb Eric Moss, Robert E. Kayen, Liyuan Tong, Songyu Liu, Guojun Cai, and Jiaer Wu. August 2009.

PEER 2009/101 *Report of the First Joint Planning Meeting for the Second Phase of NEES/E-Defense Collaborative Research on Earthquake Engineering.* Stephen A. Mahin et al. July 2009.

PEER 2008/104 *Experimental and Analytical Study of the Seismic Performance of Retaining Structures.* Linda Al Atik and Nicholas Sitar. January 2009.

PEER 2008/103 *Experimental and Computational Evaluation of Current and Innovative In-Span Hinge Details in Reinforced Concrete Box-Girder Bridges. Part 1: Experimental Findings and Pre-Test Analysis.* Matias A. Hube and Khalid M. Mosalam. January 2009.

PEER 2008/102 *Modeling of Unreinforced Masonry Infill Walls Considering In-Plane and Out-of-Plane Interaction.* Stephen Kadysiewski and Khalid M. Mosalam. January 2009.

PEER 2008/101 *Seismic Performance Objectives for Tall Buildings.* William T. Holmes, Charles Kircher, William Petak, and Nabih Youssef. August 2008.

PEER 2007/101 *Generalized Hybrid Simulation Framework for Structural Systems Subjected to Seismic Loading*. Tarek Elkhoraibi and Khalid M. Mosalam. July 2007.

PEER 2007/100 *Seismic Evaluation of Reinforced Concrete Buildings Including Effects of Masonry Infill Walls.* Alidad Hashemi and Khalid M. Mosalam. July 2007.

The Pacific Earthquake Engineering Research Center (PEER) is a multi-institutional research and education center with headquarters at the University of California, Berkeley. Investigators from over 20 universities, several consulting companies, and researchers at various state and federal government agencies contribute to research programs focused on performance-based earthquake engineering.

These research programs aim to identify and reduce the risks from major earthquakes to life safety and to the economy by including research in a wide variety of disciplines including structural and geotechnical engineering, geology/seismology, lifelines, transportation, architecture, economics, risk management, and public policy.

PEER is supported by federal, state, local, and regional agencies, together with industry partners.

PEER Core Institutions:
University of California, Berkeley (Lead Institution)
California Institute of Technology
Oregon State University
Stanford University
University of California, Davis
University of California, Irvine
University of California, Los Angeles
University of California, San Diego
University of Southern California
University of Washington

PEER reports can be ordered at http://peer.berkeley.edu/publications/peer_reports.html or by contacting

Pacific Earthquake Engineering Research Center
University of California, Berkeley
325 Davis Hall, mail code 1792
Berkeley, CA 94720-1792
Tel: 510-642-3437
Fax: 510-642-1655
Email: peer_center@berkeley.edu

ISSN 1547-0587X